NASA

National Aeronautics and
Space Administration

Lyndon B. Johnson Space Center
Houston. Texas 77058

PUBLICATION 51

MAY 1980

JSC 16671

BRECCIA GUIDEBOOK NO. 4

67015

URSULA B. MARVIN

HARVARD-SMITHSONIAN CENTER
   FOR ASTROPHYSICS
60 GARDEN STREET
CAMBRIDGE, MA 02138

Acknowledgements

TABLE OF CONTENTS

List of Figures

Rock 67015

Geologic Setting. Rock 67015 is a polymict breccia collected at Station 11 inside the rim crest of North Ray Crater (Figure 1). Rocks from this location are of special interest because North Ray Crater (∿1000 m diameter; 230 m deep) is the deepest excavation into the highlands crust visited by astronauts on any mission. Exposure ages on samples of ejecta indicate that the crater is only about 50 m.y. old (Marti et al., 1973). This age conforms with the youthful appearance of the crater, which exposes several stratigraphic layers in its walls (Figure 2). The crater penetrates into dark colored rocks that are the probable source of some dark boulders on the crater floor and of dark matrix breccias lying on the outer rim. The dark layer is overlain by light colored formations that yielded specimens of light gray breccias such as 67015.

North Ray Crater lies on a ridge that may be a downfaulted block of Smoky Mountain. If it is, the upper layers exposed in the crater probably represent the bedrock of the Descartes mountains (Ulrich, 1976). Alternatively, the light colored upper layers may be Cayley plains material and the darker layers the bedrock of Smoky Mountain (Hodges, et al., 1973). By either inter- pretation the clasts in the breccias from North Ray Crater constitute a promising hunting ground for samples of the ancient highlands crust.

Macroscopic Description and Classification. Rock 67015 was a large, loose specimen collected in the "interboulder" area of the rim. (The inter- boulder area was a relatively rubble-free zone lying between House Rock and the White Boulder area). The original specimen was approximately 13 x 10 x 8 cm and weighed 1194 grams. The most conspicuous features of this rock are large, irregular, dark gray clasts in a light gray matrix (Figure 3). The

1

Figure 1. Two sketch maps showing the geologic setting of station 11 on the rim of North Ray Crater and the site where 67015 was collected. (A. Modified from Ulrich, 1976, Figure 2). (B. Modified from Ulrich, 1976, Figure 13).

A.

0 — 500
m

North Ray Crater

Dark Boulders →

Smoky Mt.

←El. 7975m

0 \House Rock

Station 11 ●

Interboulder Area

Kiva Crater

White Breccia Boulders →

North Ray Ridge

B.

North Ray Crater

67015
67055
67095
67115

White Breccia Boulders:
  67455
  67475
  67605
  67610
  67600

Crater Rim

0 — 50
m
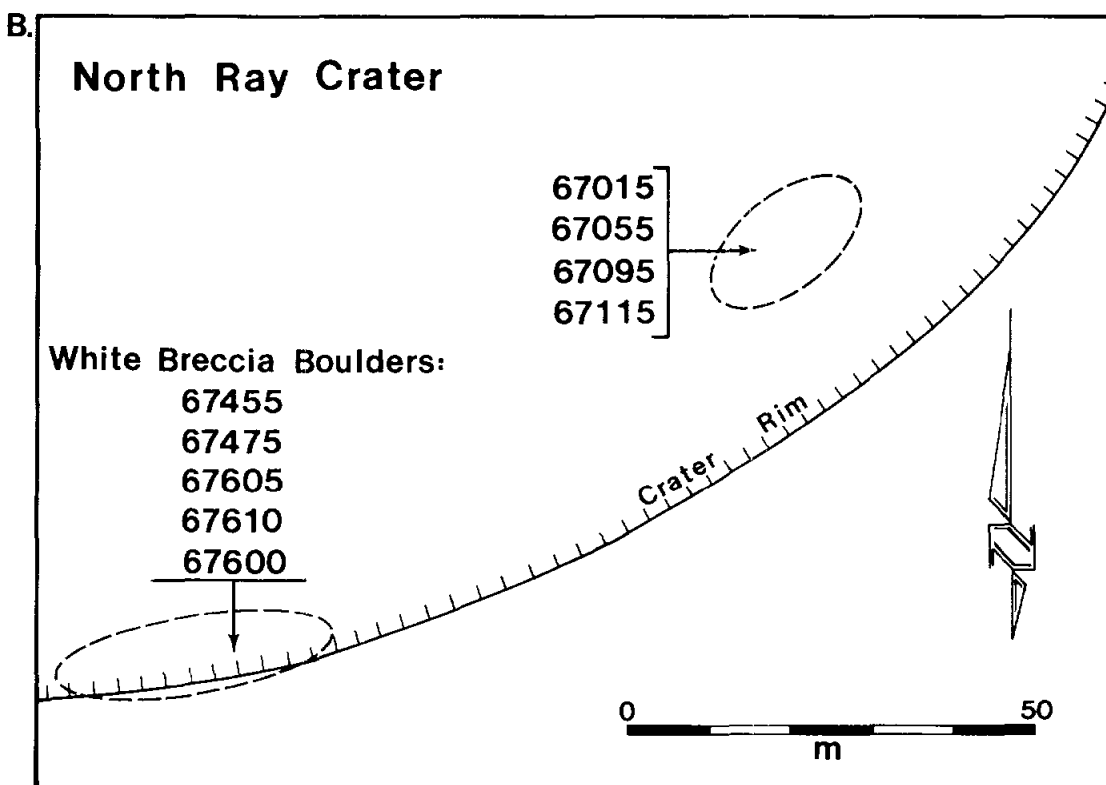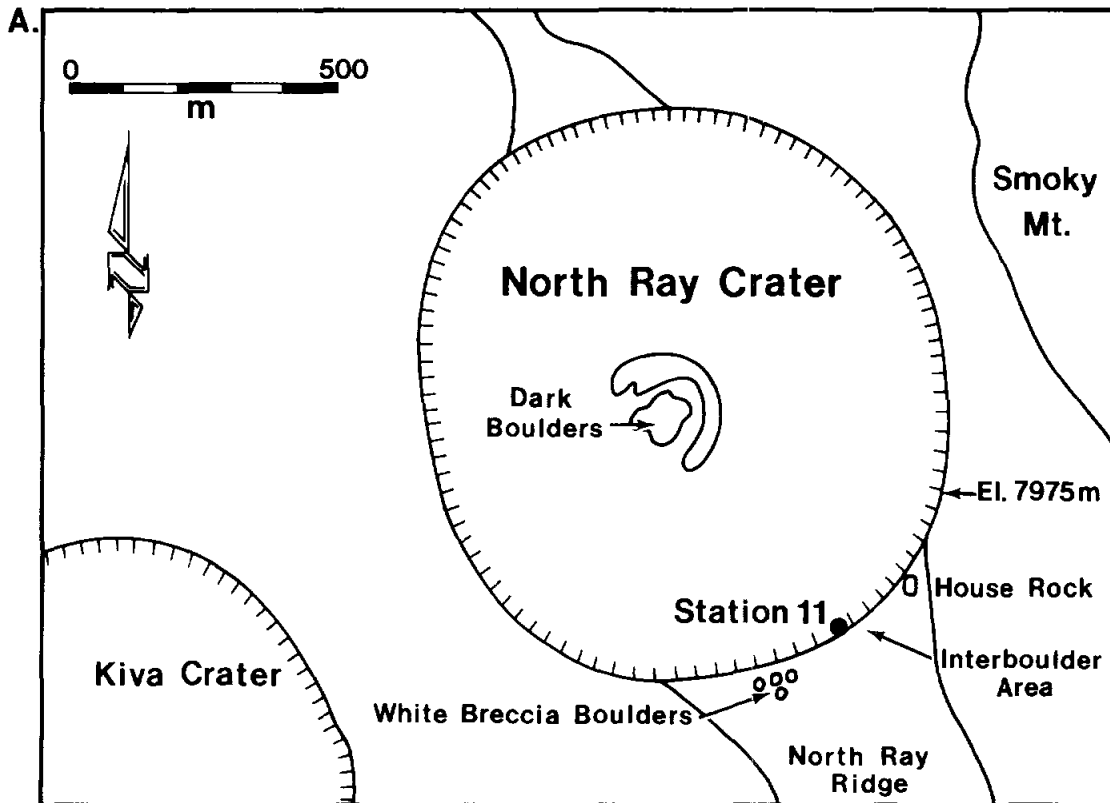
Figure 2. Hypothetical stratigraphic section through North Ray Crater (modified from Ulrich, 1973, Figure 5).

W ———————— E

Smoky Mt.

?

Ejecta

Light matrix
◄— breccia

Dark matrix
◄— breccia
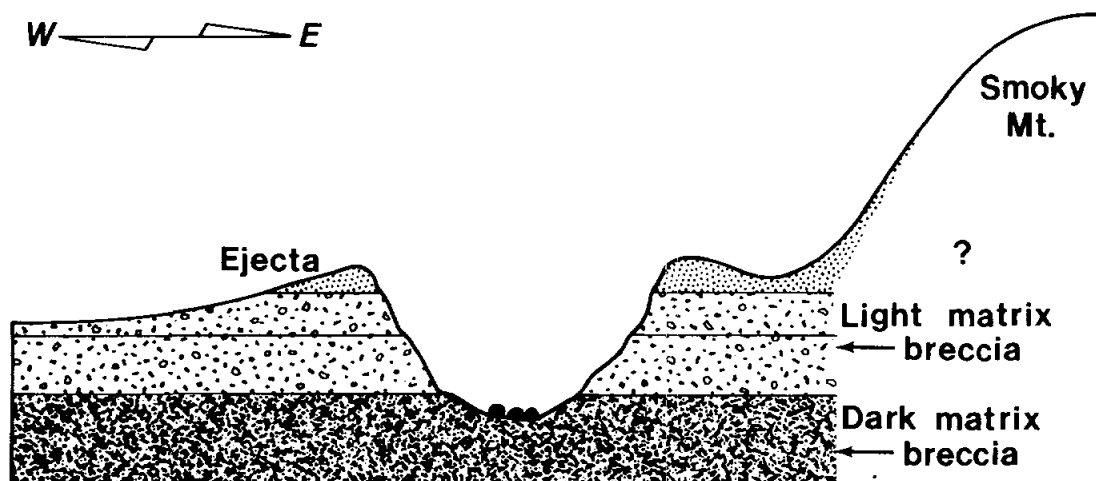
matrix is friable and easily sheds clasts, both large and small, leaving
the surface pitted with clast molds. Several major cracks penetrated the
rock making handling without breakage difficult.

67015 was originally classified by Wilshire, Stuart-Alexander, and
Jackson (1973) as a B_2 (light matrix-dark clast) breccia. They speculated
that 67015 might have been formed by the brecciation and reconstitution of
rocks similar to the black and white Apollo 15 specimens (15455 and 15445),
which have white clasts in a dark, aphanitic matrix. They suggested that
B_2-type breccias and the white soils at the Apollo 16 site were created by
a series of local impact events that occurred before the formation of North
Ray Crater.

Because it contains small amounts of glass in the matrix and among the
clasts, Wilshire, Stuart-Alexander, and Schwarzman (1976) reclassified 67015
as a $B_3(B_2)$ breccia characterized by an intermediate matrix color with light
and dark clasts. These authors describe 67015 as possibly a loosely aggregated,
complex soil breccia from the highland regolith.

Processing. The initial subdivision of 67015, in 1972, is depicted in
Figure 4. Several chips were taken from the main mass. Three of them (,4 ,5
,6) were potted and made into polished thin sections (,8 ,9 ,10 ,25 ,26 ,27).
The west end of the specimen broke along preexisting cracks producing sub-
samples ,2 and ,3 (later renumbered to ,16 and ,17). These in turn yielded
the 19 subsamples listed in the figure.

The first (and only) saw cut on 67015,0 was begun on October 2, 1975.
The friability of the matrix caused sizeable pieces to break off and numerous
clasts to fall out. There resulted an abundance of fines. The sawed
surfaces on each end piece (,0 and ,57) were plucked and coarsely
corrugated. Cracks widened until 67015,0 split in three pieces: 67015,0

4

Figure 3. Three views of 67015 at the Lunar Receiving Laboratory, 1972.
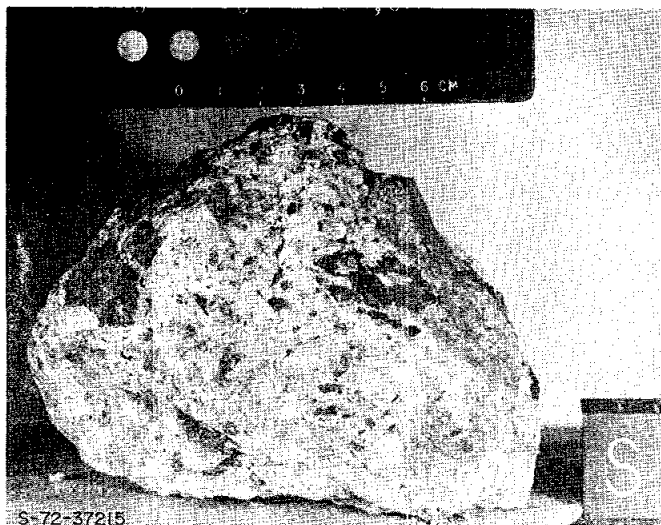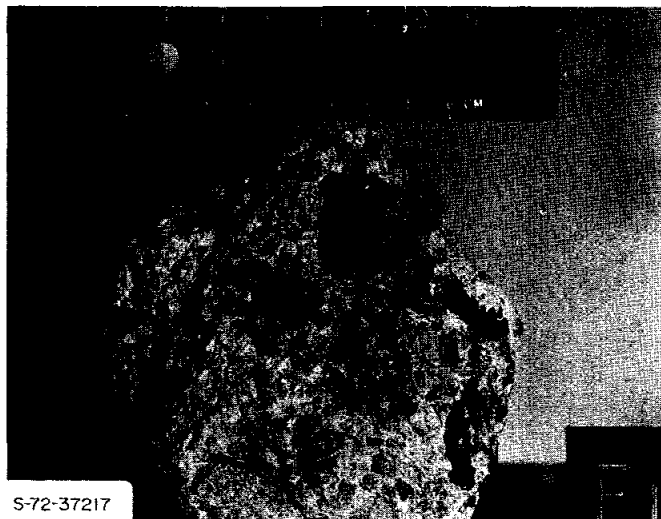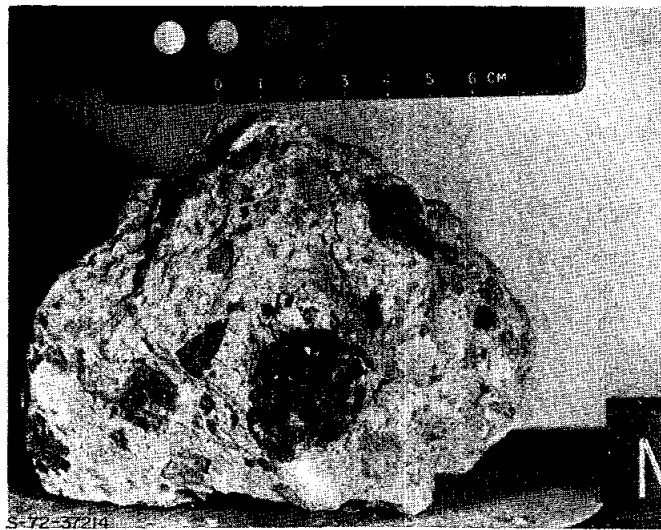
Figure 4. The chipping of lunar rock 67015.
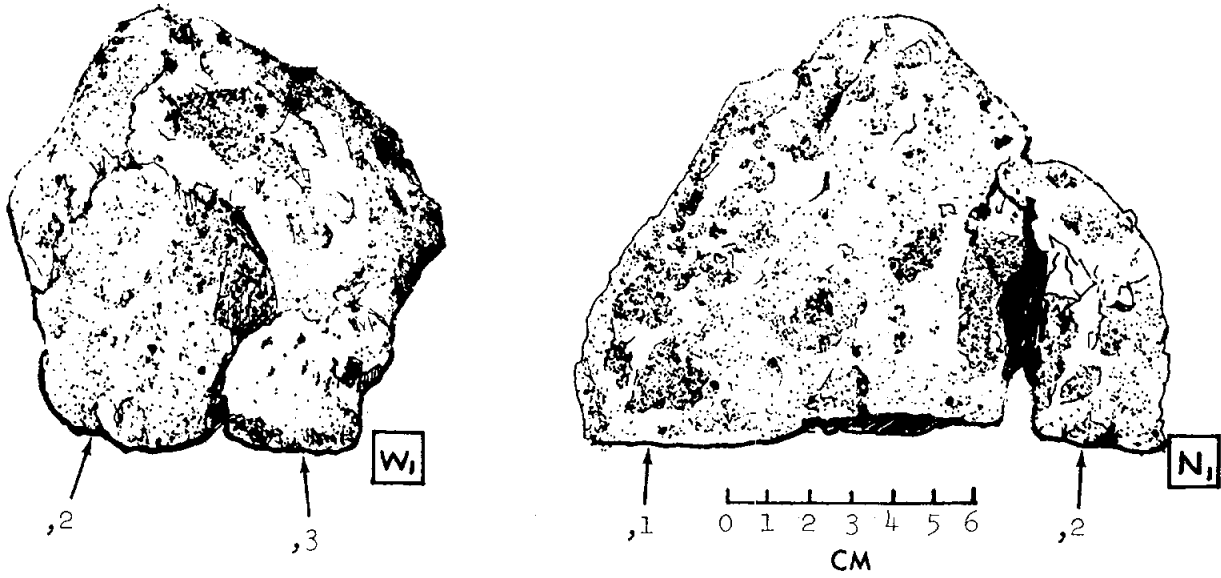
T_1 Reference (only) orientation used
for LRL photography.

6
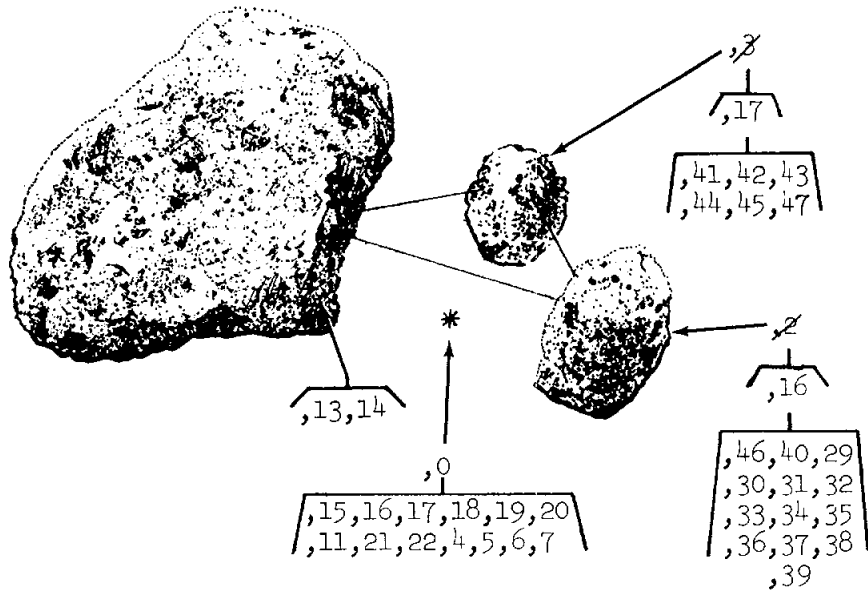
Figure 5. The sawing of 67015.

    A. The initial saw cut on 67015,0, October 2, 1975.

    B. Final result of sawing 67015,0, October 8, 1975: Sawed surfaces of 67015,57 (W_1) and 67015,64 (renumbered from 67015,0) (E_1). 67015,58 broke away from ,64 along a pre-existing crack.
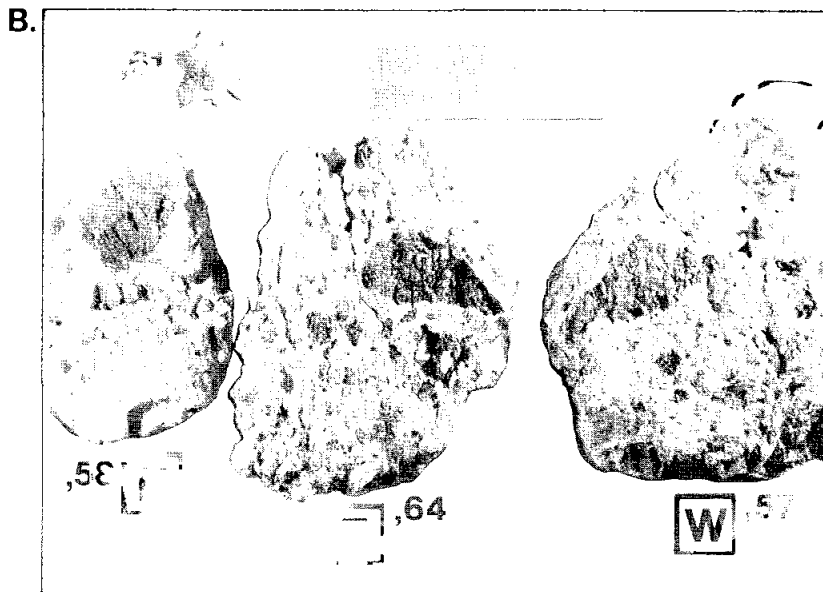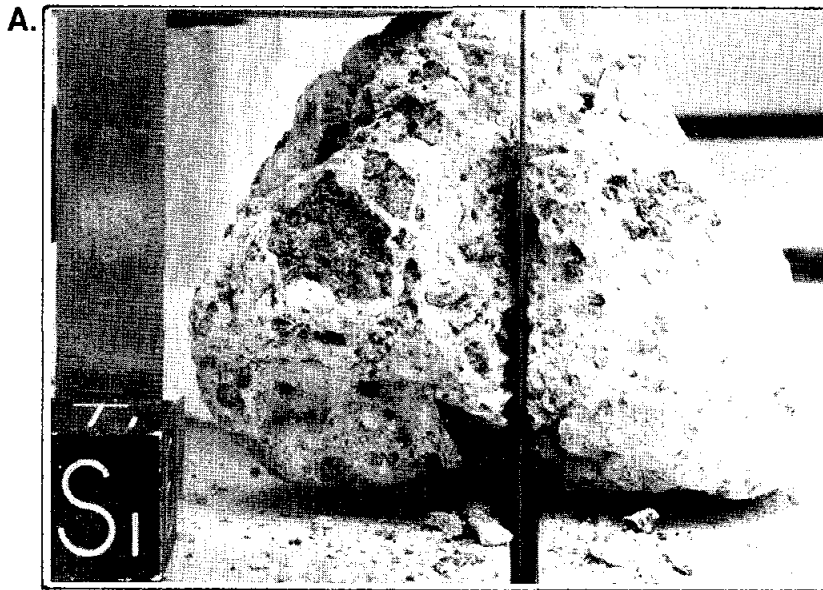
(renumbered to 67015,64), 67015,58, and 67015,61 (Figure 5).

The largest single subsample, 67015,57 (342 g) is the main mass described in this Guidebook. The second largest 67015,64 (340 g) lies in storage in Brooks Air Force Base at San Antonio.

67015,57: The East End

Photographs and maps of this sample are shown in Figures 6 and 7. The sample weighs 341.7 grams. It has one sawed surface (W_1); the remainder were exterior surfaces although most of them are now difficult to recognize as such because dusting and handling have caused a grain-by-grain loss of material as well as the considerable loss of chips and clasts. Few zap pits remain visible and there are only traces of brown dust which originally covered large areas of the surface.

The Matrix. The matrix of 67015,57 is a light gray, porous, friable aggregate of mineral fragments. Some zones are moderately coherent, presumably as a result of various degrees of annealing. The matrix consists of about 95% plagioclase, 4% olivines and pyroxenes, traces of ilmenite, metal and sulfide grains, pink spinel, and sparse glass.

Clasts. In addition to monomineralic fragments of plagioclase, olivine, and pyroxene, five types of lithic clasts are visible in the hand specimen. These are designated on the basis of color and texture, as DG (Dark Gray Aphanitic), G (Gray Aphanitic), GC (Gray Crystalline), W (White), and B (Basaltic).

DG (Dark Gray Aphanitic) Clasts. These are dark, finely vesicular, aphanitic materials ranging from 1 mm grains to large, lobate masses over 6 cm long. Eight clasts of this type are numbered on the maps of Figure 7. A few small ones are indicated by the symbol but are not numbered, and many more, 1.0 to 3 mm in size, are not mapped. The clasts have rough jagged surfaces and irregular outlines. They are tough and brittle.

DG-1 is the largest clast of this type. It can be seen in all of the maps except W_1, as it spreads tentacle-like over the surface. Clasts such as DG-1 and DG-2 appear to be aggregates of numerous small clots of the dark

9

Figure 6. Lithologic maps of the photographed surfaces of 67015,57

Clast Fragments from Large Clast Mold on ⊢

KEY

DG
Dark Gray Vesicular Aphanites

G
Gray Massive Aphanites

GC
Gray Sugary Crystallines

W
Anorthositic Clasts

B
Basaltic Textured Clasts

Patina

Clast Molds
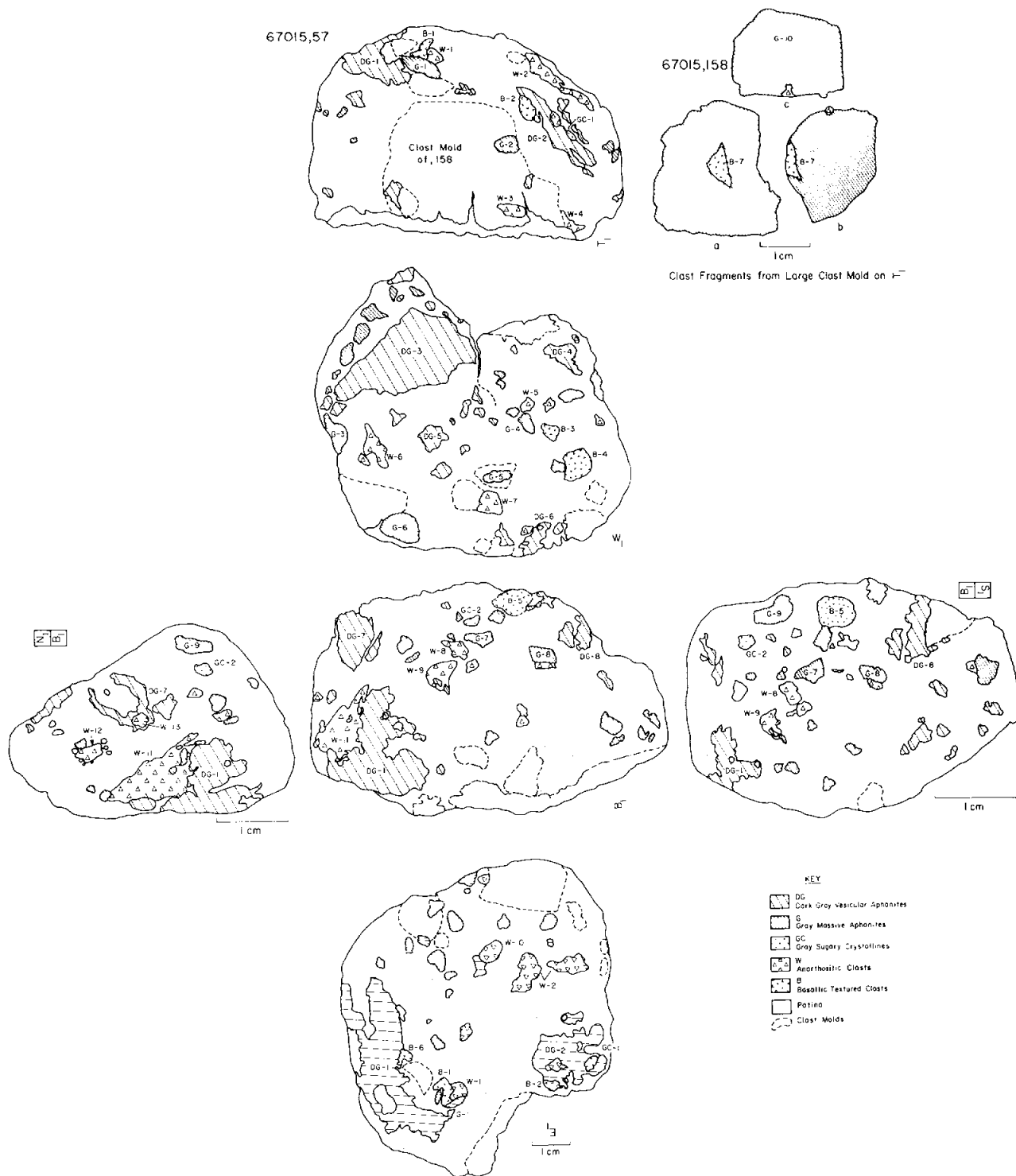
Figure 7. Surfaces of 67015,57. Refer to Figure 6 for the key.

Figure 7a. Surface T₁

S-79-31998

67015, 57

Figure 7b. Surface W$_1$

S-79-31997

67015, 57
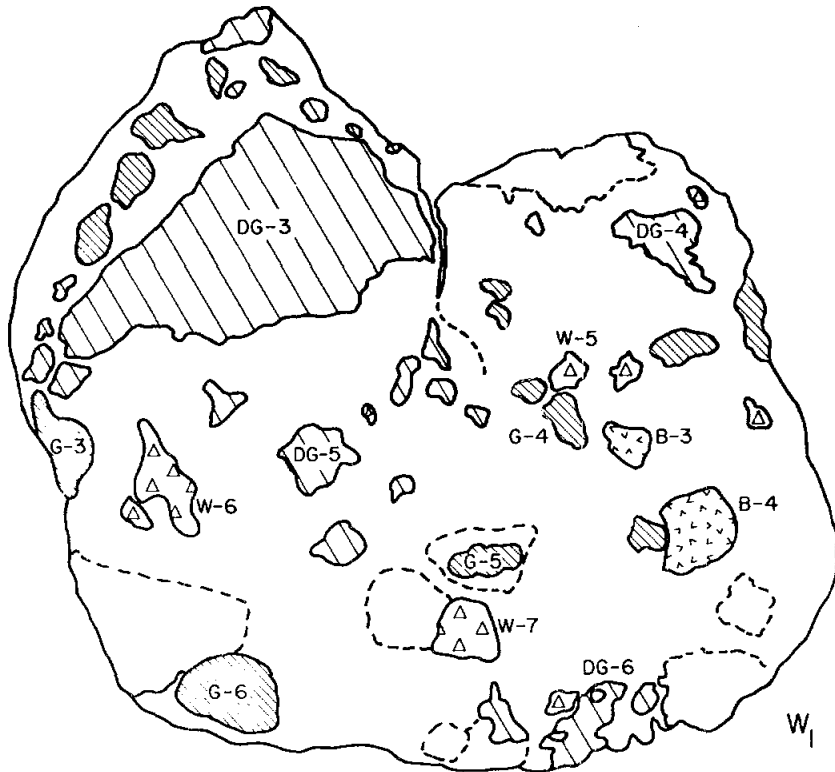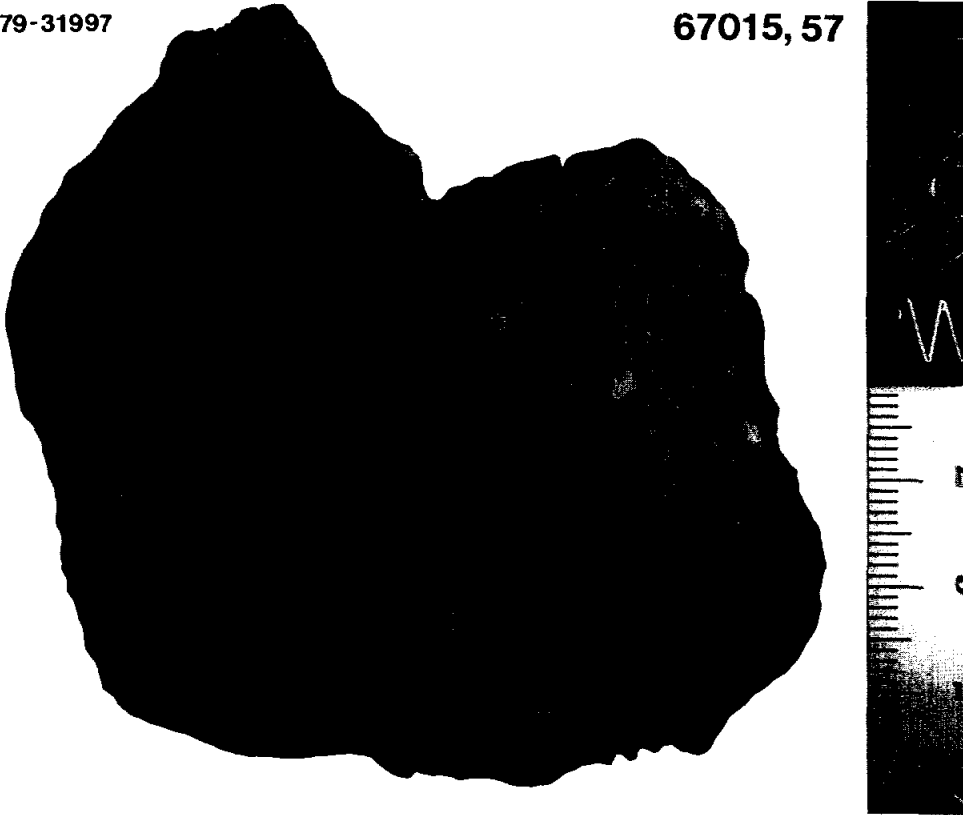
Figure 7c.   Surface B₁

67015, 57
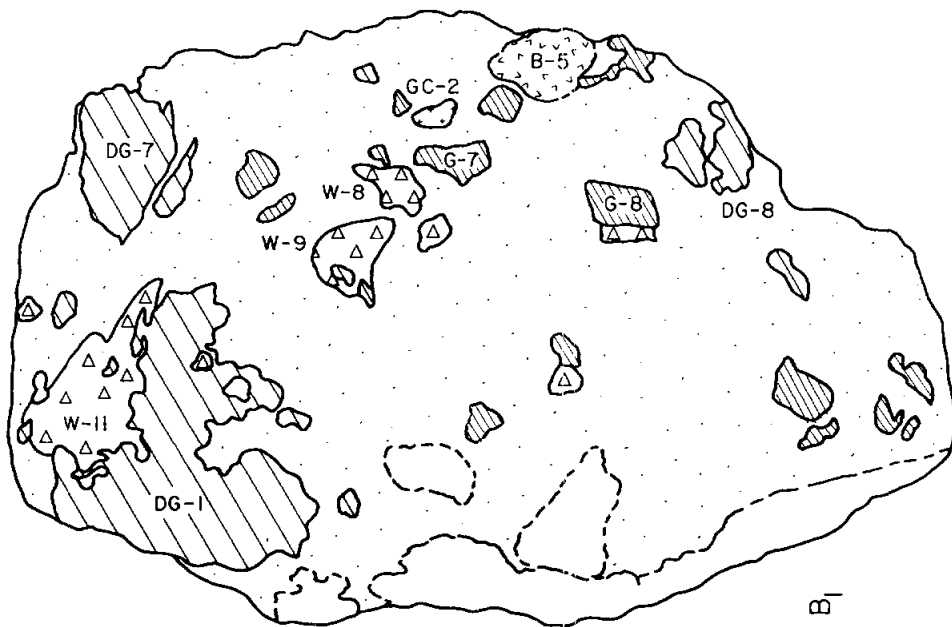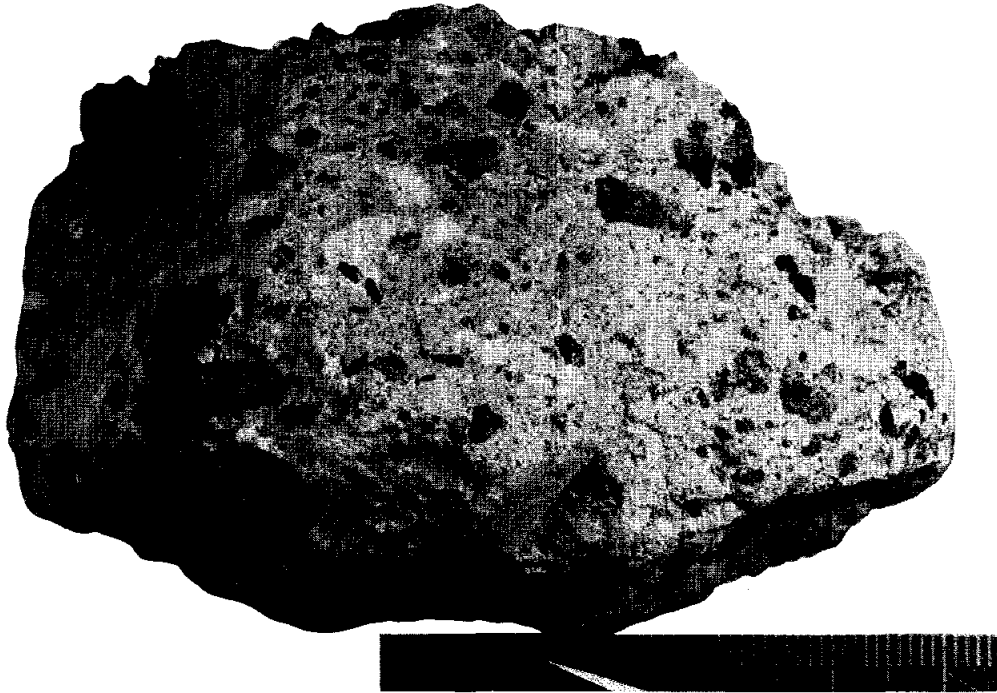
Figure 7d. Surface N_1-B_1

67015, 57   S-79-34539

67015, 57

1 cm
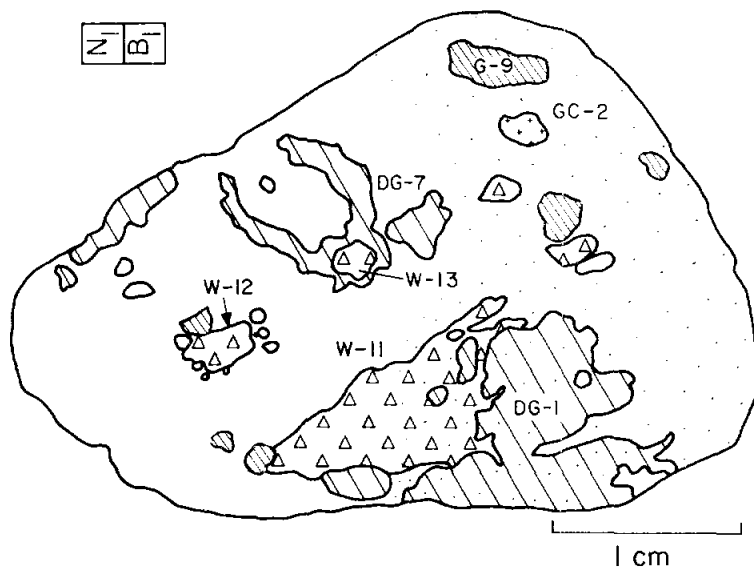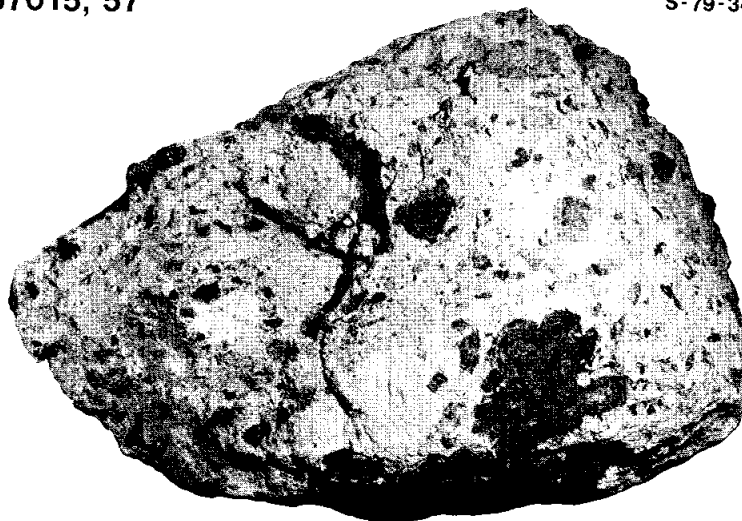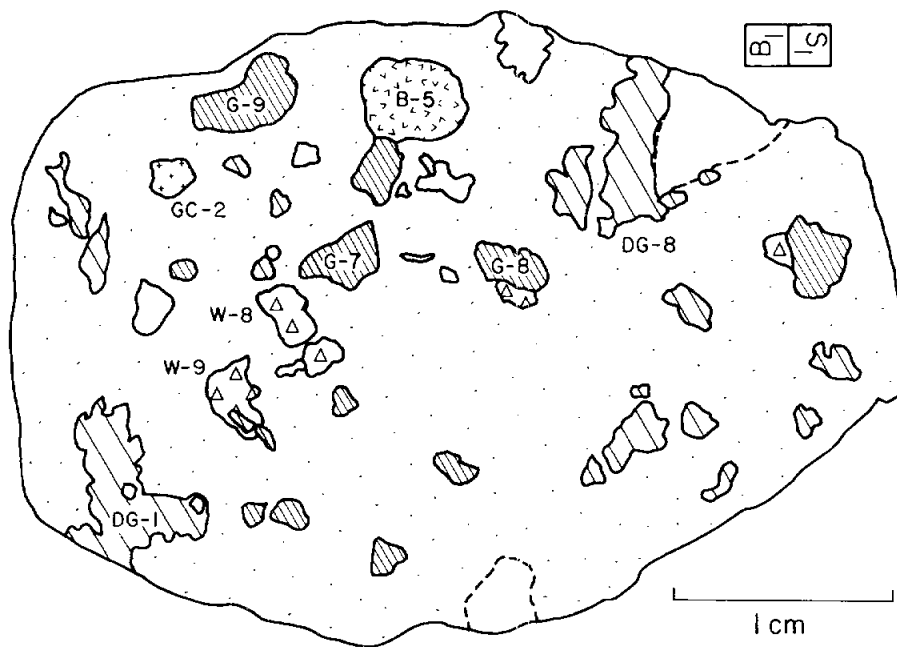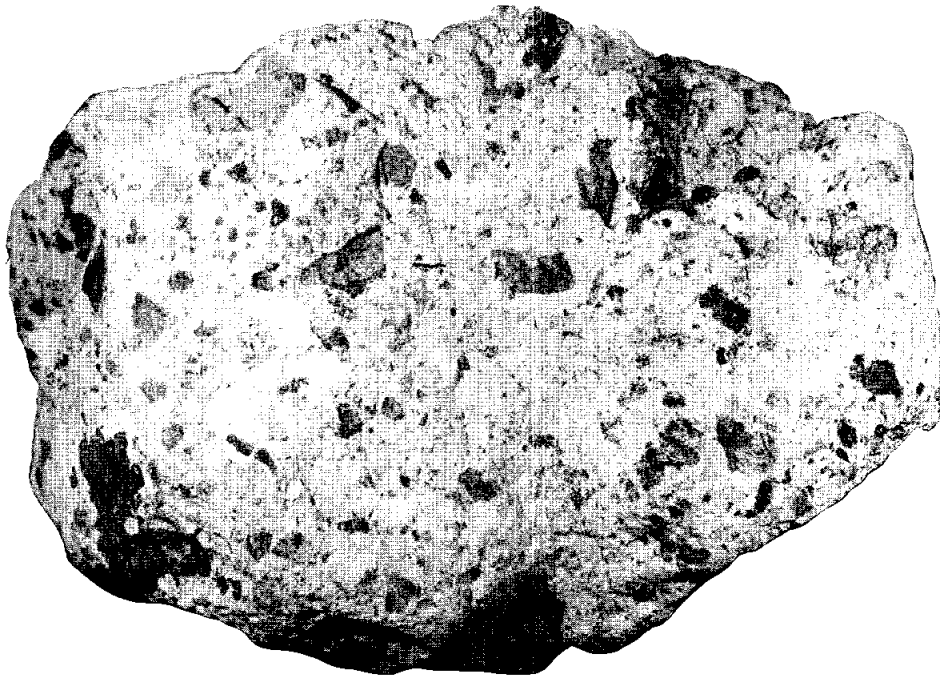
Figure 7f. Surface E$_1$

67015, 57

S-79-32001

1 cm

67015, 57

,158

S-79-31999

67015,158

G-10

c

B-7

B-7

a

b

1 cm

Clast Fragments from Large Clast Mold on ⊢⁻
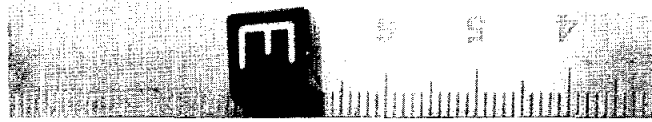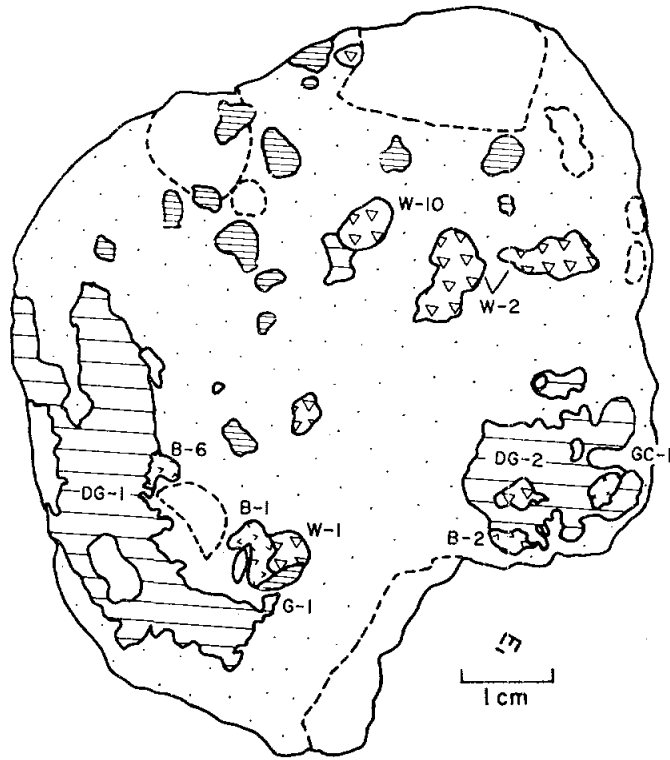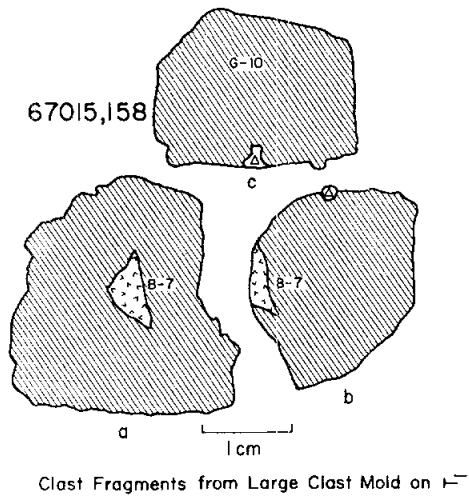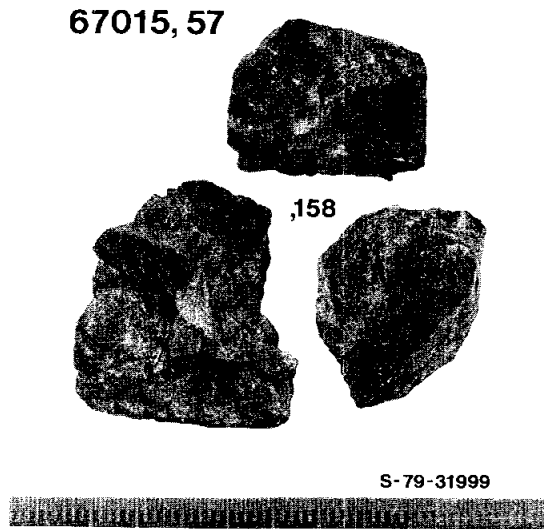
material massed together in free forms that sometimes enclose patches of matrix. Clast DG-3 is one of the more compact examples. DG-7 is a remnant of a much larger clast that fell out during the mapping. All of the DG clasts incorporate small white fragments visible to the naked eye. This vesicular dark gray rock is clearly a breccia--most probably an annealed fragment-laden impact melt--with a very dark matrix. All of the DG clasts appear to be of similar material. Any of them would be easy to pry from the matrix, but dark clast fragments selected from the fines of 67015 would probably serve equally well for thin sections and analyses.

G (Gray Aphanitic) Clasts. These are medium gray, massive, non-vesicular clasts up to 2 cm in size. They are tough, angular, and blocky with smooth surfaces. They differ strikingly from the rough, vesicular, and generally much larger DG-type clasts. The G clasts are aphanitic but include some small, generally inconspicuous light colored fragments. They are clearly annealed breccias.

The larger G clasts are numbered in the maps; many more smaller ones occur in the rock. The large (2-3 cm) clast 76015,158, which fell in three pieces out of the clast mold on the T_1 surface of 67015,57 is of this type. It is large enough,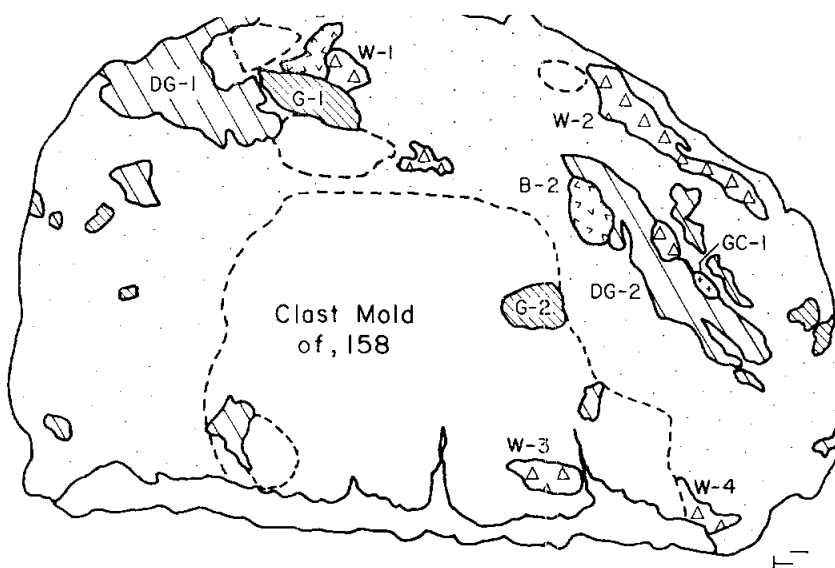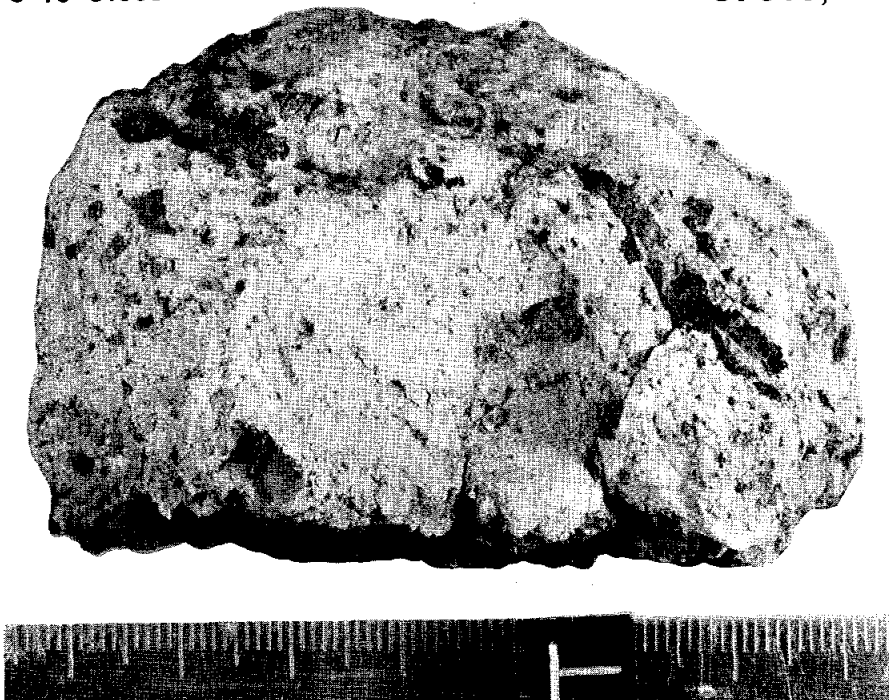 however, so that some variations in texture occur. It possesses a very few minute vesicles with crystals inside them. Sparse brown pyroxenes and light gray plagioclase fragments are visible in the groundmass. One 0.5 mm inclusion of translucent plagioclase occurs on the "c" fragment (see Figure 7), and pieces of a 7 mm brownish-yellow clast (B-7) of fine grained "basalt," which occurred in the center of the 67015,158 clast, are attached to the "a" and "b" fragments.

GC (Gray Crystalline) Clasts). Clasts of this type are fine to medium grained crystallines with a sugary texture. Only two of them occur on 67015,57 (see surfaces B_1 and E_1). Previously studied lunar particles of similar appearance have often proved to be noritic in composition, but there is no assurance that these will. Thin section examinations are needed to determine whether the GC clasts are a distinct chemical type, or are coarser textural varieties of the common G clasts. As another possibility, they may be related to the igneous-appearing basaltic clasts in 67015.

W (White) Clasts. The white clasts vary in texture: some resemble pulverized, compacted chalk, others have angular gray or white plagioclase fragments in a chalky groundmass, still others appear to consist of large single crystals or of coarse polycrystalline intergrowths of plagioclase. These clasts are about 100% plagioclase with or without a few grains of metallic iron, pink spinel, or mafic minerals. The clasts clearly represent anorthosites in a wide range of crushed and recrystallized textures. The majority are 6 mm across or smaller, but a few (see Clast W-11 on surface B_1N_1) form irregular masses of up to 1.5 cm. Clast W-1 is chalky but encloses two dark streaks of crushed brown material--probably pyroxene but possibly dark matrix. Clast W-11 includes a few yellow grains. Most of the others consist of angular white or translucent feldspar fragments in a chalky matrix.

B ("Basaltic") Clasts. These are fine to medium grained crystalline clasts, from about 3 to 12 mm in size, with igneous textures. All of the B clasts examined to date are rich in plagioclase (55-75%) and have 25-45% olivines and pyroxenes with or without sparse ilmenite or metal grains. The coarser grained clasts are very friable; finer grained ones are coherent.

Most of these clasts may be crystallized impact melts. However, rocks such as 67015 are of special interest because of the possibility that they may contain clasts of eruptive igneous rocks including mare-type lavas of Preimbrian age.

The largest of the B clasts are B-4, B-5, and B-7. Clast B-4 is a thin remnant, about 6 mm across, of a larger clast that was cut or broken away during the sawing of the W_1 surface. It consists of approximately 65% plagioclase in crystals 0.7 to 2 mm long, and 35% yellow mafic grains up to 0.4 mm across. Also present are one or two pinpoints of an opaque mineral. Clast B-5 is about 8 cm across and is about 65% plagioclase in 1 mm grains, 25% yellow olivine (?) and 10% cinnamon pyroxene (both about 0.5 mm), and 1% opaques. B-7 is a clast of fine-grained yellow and brown mafics (50%) and feldspar (50%) that occupied the interior of the large gray aphanitic clast (67015,158). It will be interesting to learn whether the aphanitic G-clast and its principal inclusion, B-7, are both impact melts similar in composition but differing in texture.

67015,58 and its Descendants.

67015,58, from the west end of the original specimen (,0), was completely subdivided to produce subsamples 67015,161 to ,168 (Figures 8 and (9).

67015,161. (43.98 g.) This is the largest subsample of 67015,58. Photographs and maps of 67015,161 are shown in Figures 10 and 11. All five clast types occur on this subsample. The most striking clast is B-10, a 1.5 cm basaltic fragment consisting of 65% plagioclase crystals 1-2 mm in size, and 35% yellow mafics up to 1 mm in size. No brown pyroxene or opaques are visible. A chalky white rim surrounds B-10 and penetrates it along curving cracks. Two smaller B-type clasts (B-8 and B-9) also occur on this specimen. B-8 is embedded in a mass of chalky anorthosite. One sugary gray crystalline clast (GC-3) is visible on the edge of the T_1 surface. Several DG and G clasts are shown on the maps.

In September, 1979, 67015,210,a subsample including clast B-8, was chipped from 67015,161 (Figure 12). This piece was returned to storage without further subdivision.

Figure 8.   Sketch of the main subdivisions of 67015,0 and of 67015,58.

,0   ,57   ← This guidebook-
            main mass

,58
,64 ←Brooks Air Force Base
,61
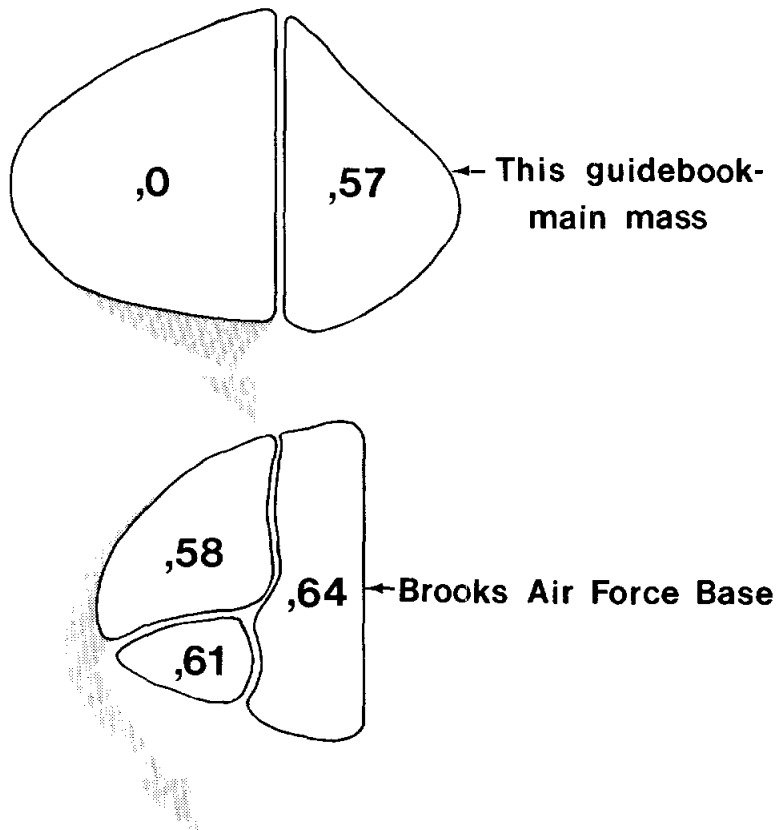
,161   ,162   ,163   ,164
43.9g   31.1g   16.8g   4.1g
>1cm   >1cm   >1cm   4-10mm

,165   ,166   ,167   ,168*
3.0g   2.0g   6.6g   0.8g
2-4mm   1-2mm   <1mm   1-10mm
                        (in dish)

*Basaltic clasts handpicked from 1-10mm
fines

22

Figure 9. Group photograph of the subsamples of 67015,58: 67015,161 to 67015,168.

S-79-31340

,161   ,162

67015.58
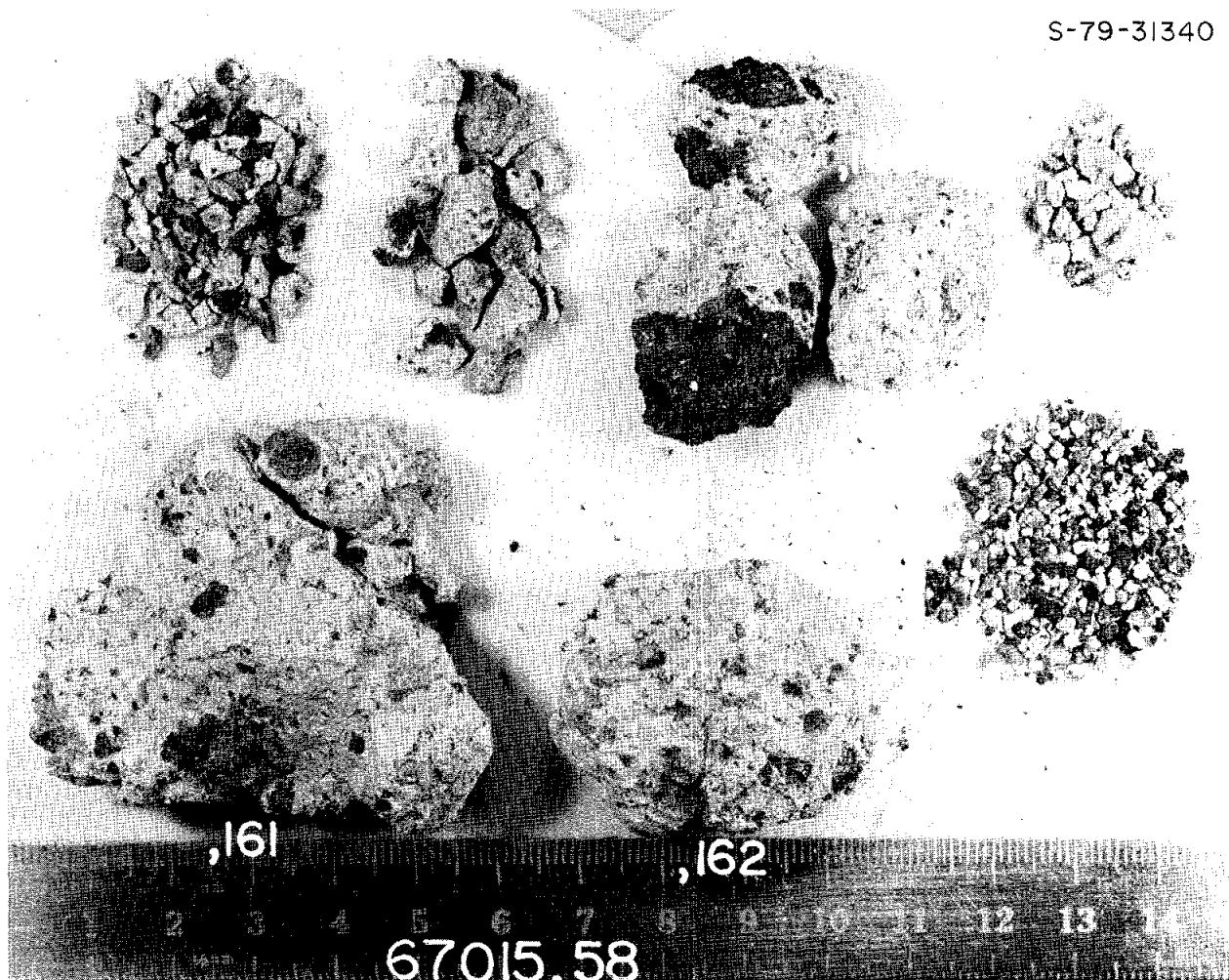
Figure 10. Sample 67015,161; top and bottom views.

67015, 161

1 cm

T₁

67015, 161

B₁

1 cm
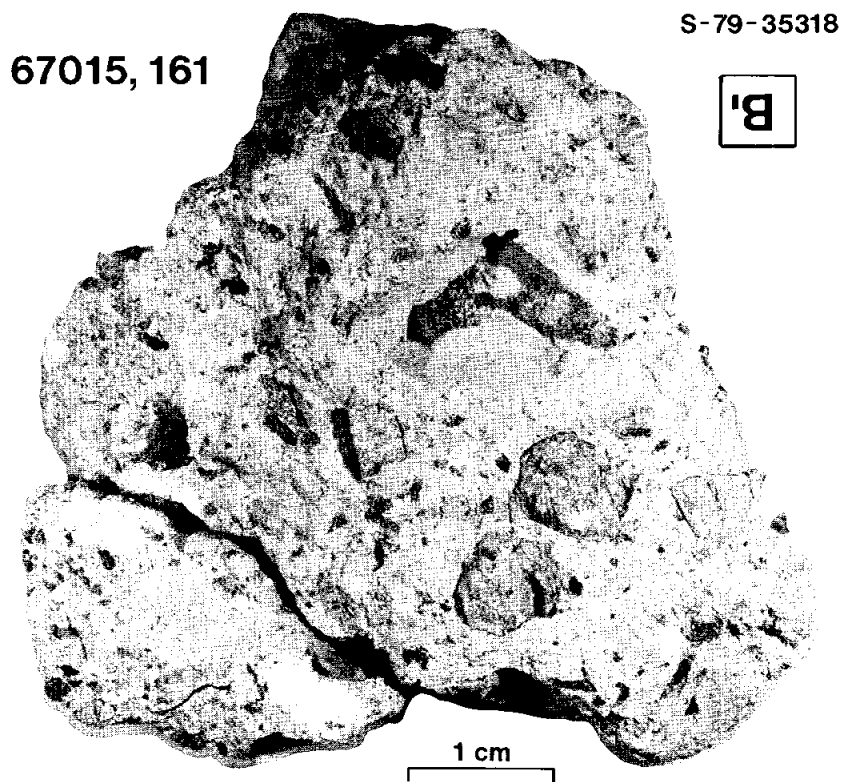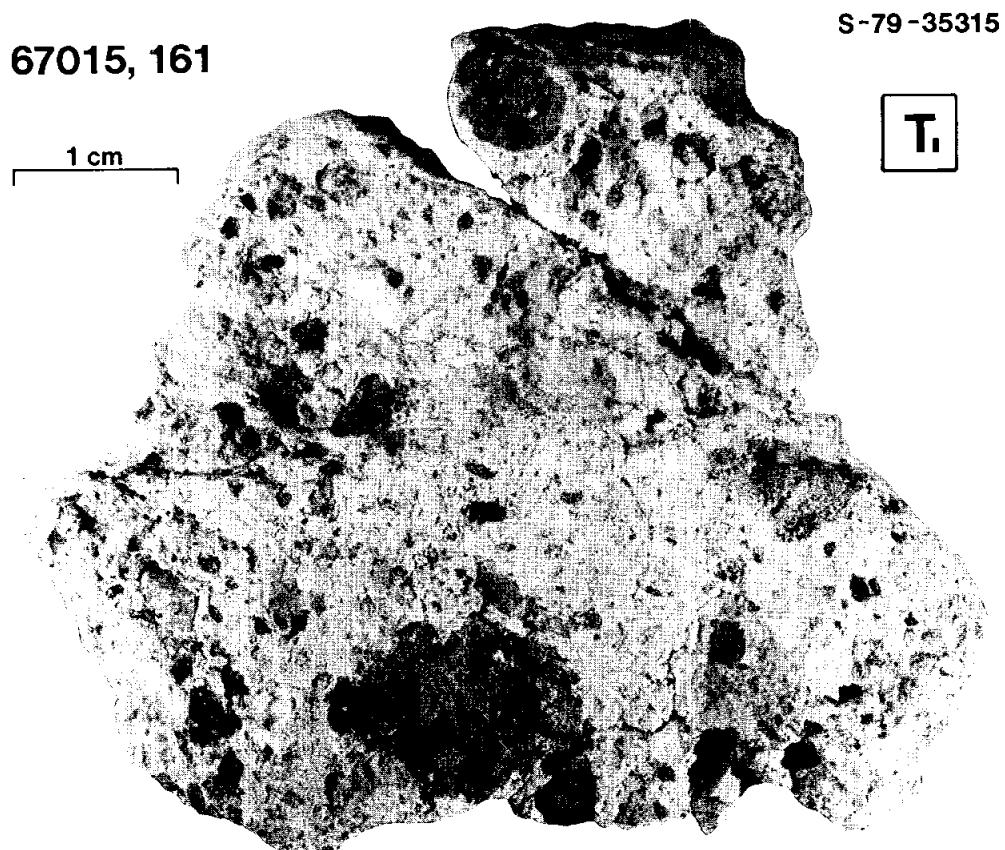
Figure 11. Surface maps of 67015,161.

67015, 161
T₁

67015, 161
B₁

KEY

DG
Dark Gray Vesicular Aphanites
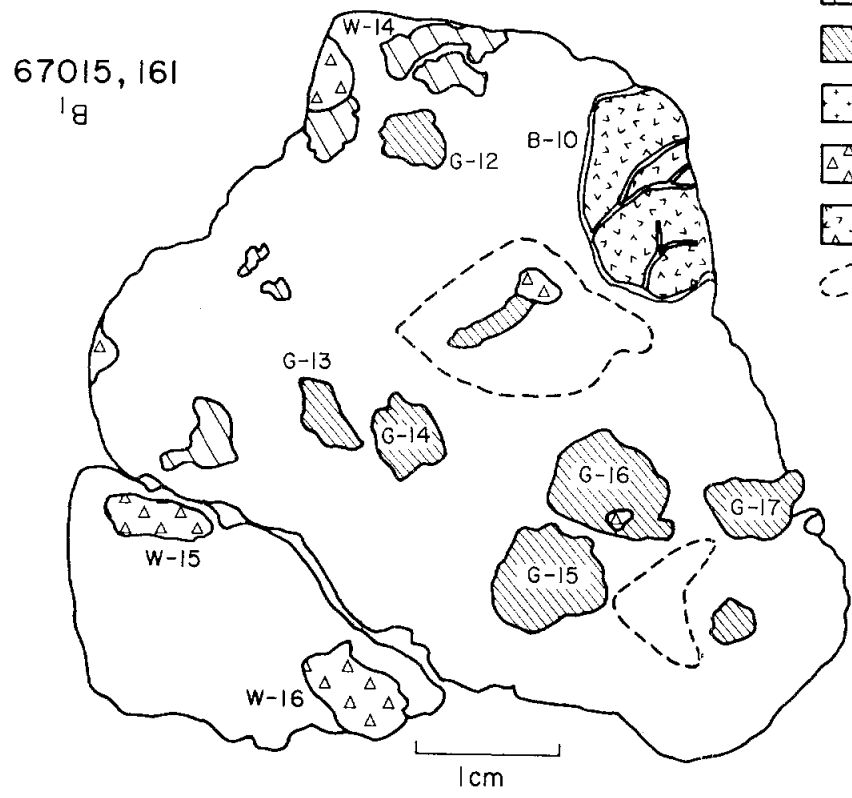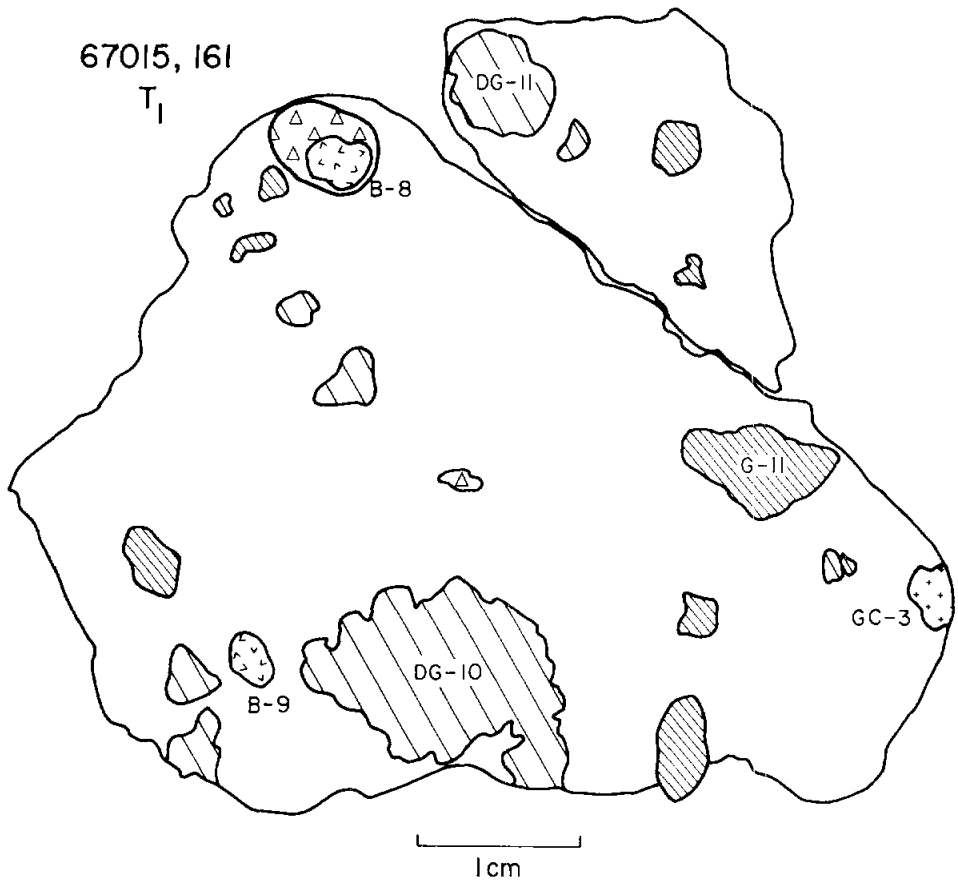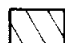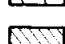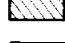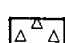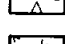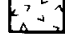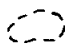
G
Gray Massive Aphanites

GC
Gray Sugary Noritic Crystallines

W
Anorthositic Clasts

B
Basaltic Textured Clasts

Clast Molds

Figure 12.   Sample 67015,161 was subdivided to produce 67015,210, a
   piece that includes basaltic clast B-8.
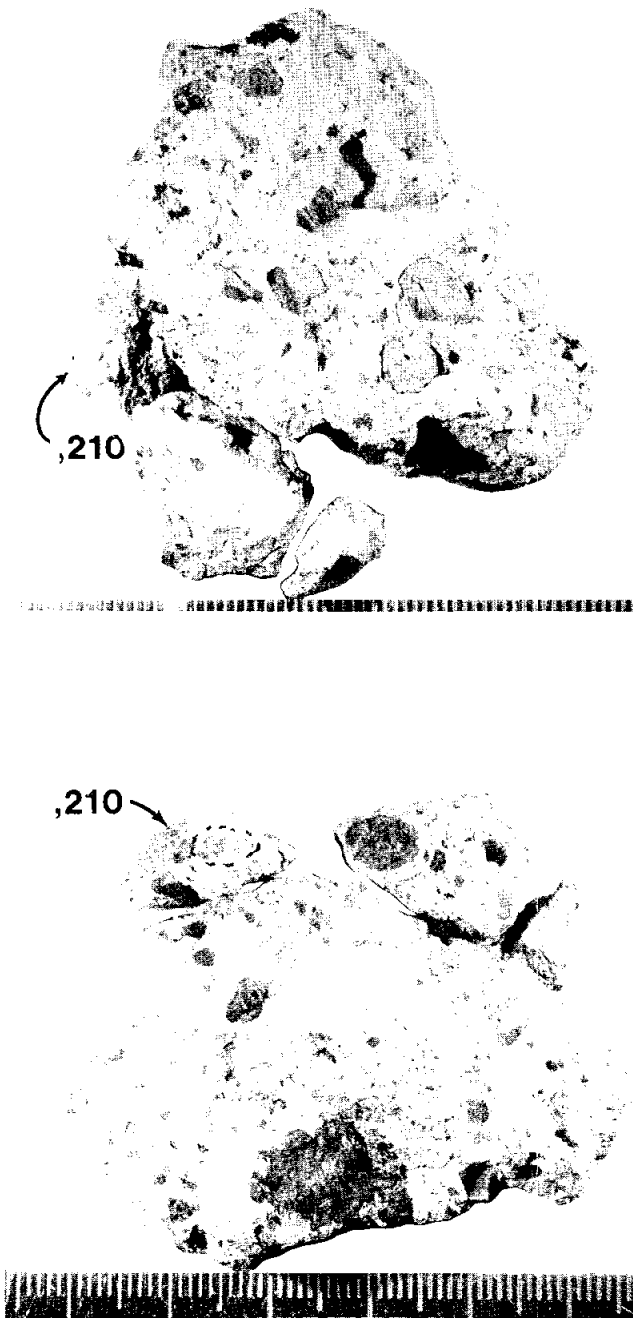
67015,162. (31.14 g.) This piece (Figure 13, 14) is dominated on one surface by a 3-cm dark gray vesicular clast (DG-12), which contains a few conspicuous white feldspar fragments. The other surface exhibits a basaltic clasts (B-11 and B-12). B-11, the larger of the two, is about 1 cm across. It consists of about 65% plagioclase in 1-mm crystals, one or two of which have tiny opaque inclusions, and 35% are pale yellow pyroxene in smaller (0.4 mm) grains. No intergranular opaques are visible. Part of the clast is enclosed by a chalky rim.

Clast GC-4, a small sugary gray fragment, occurs on the T_1 surface.

Figure 13.   Sample 67015,162; top and bottom views.

Figure 14.   Surface maps of 67015,162.

67015, 58
,162
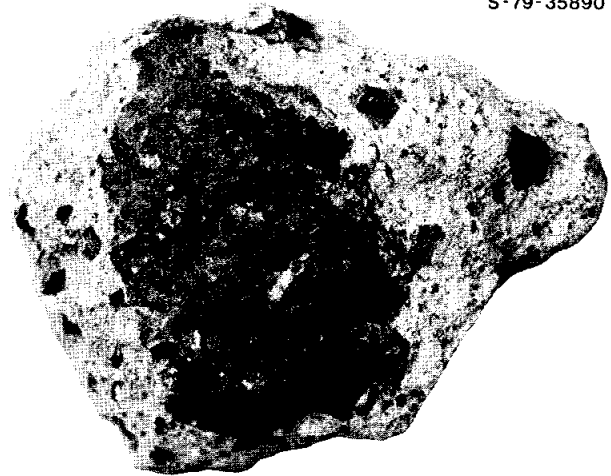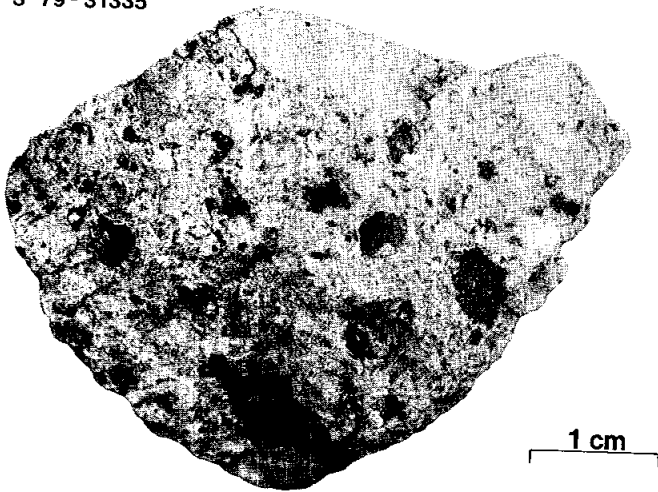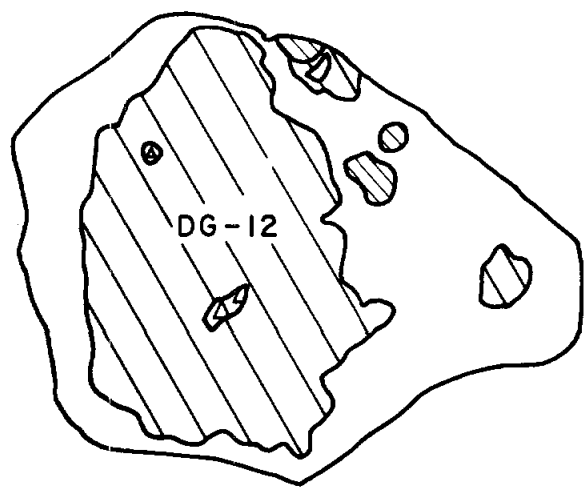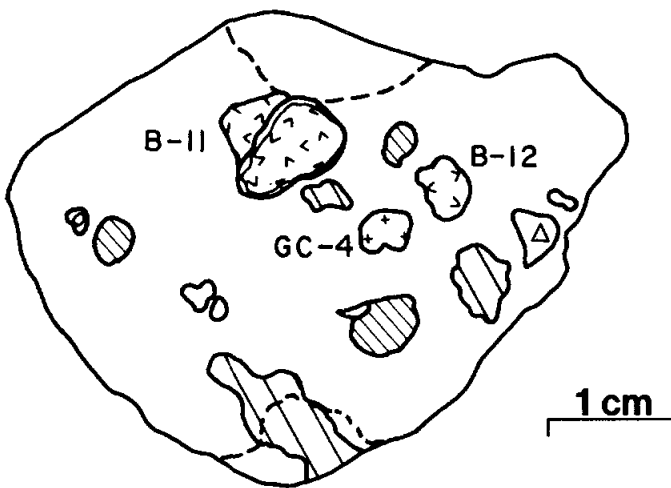
67015,163 a, b, c. Three exterior chips (a, b, c) from ,58 are shown in Figures 15 and 16. The most prominent clasts in all three pieces are typical DG-type, very rough and vesicular with small white and brown inclusions. A slight patina and a few zap pits are visible on the dark clast in c and on the matrix of b. 67015,163c would be a good source of material of this type for any study in which an exterior surface chip is acceptable. There are some small G (massive gray) clasts in piece b, but no crystalline clasts in any of the three chips.

Sample 163a was renumbered 67015,207 and chipped to produce 67015,208, a 0.211-gram black and white fragment (Figure 17). 67015,208 was potted and sliced for thin section 67015,215 (Figure 18).

Figure 15.   Sample 67015,163; three exterior chips from ,58.

Figure 16.   Maps of the photographed surfaces of sample 67015,163.

67015, 58

a   b   ,163   c

67015, 163

1 cm

Dark gray clasts
Gray clasts
⊛   Zap pit
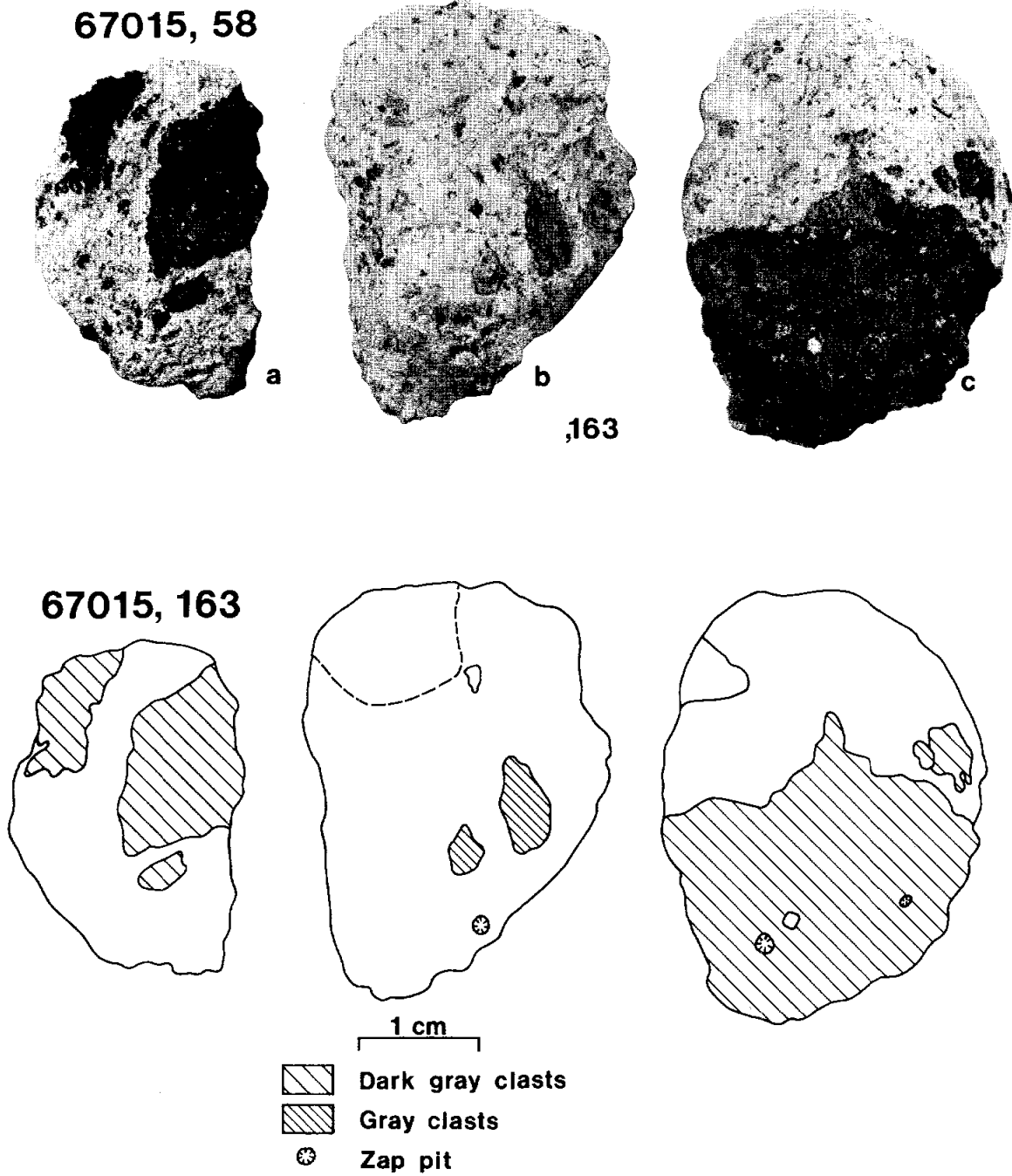
Figure 17.   The chipping of 67015,163 (renumbered ,207) to produce ,208,
   which was sent to the thin section laboratory, potted and sliced to
   thin section ,215.

Figure 18.   Thin section 67015,215 shows that the dark gray (DG) vesicular
   material is typical dark matrix breccia which occurs as rounded blobs
   and irregular, lobate masses within the porous, light gray matrix of
   67015 and numerous other light matrix highlands breccias.   (Plane
   polarized light.)

67015   S-79-36317

,207

1 cm   ,208

125µ
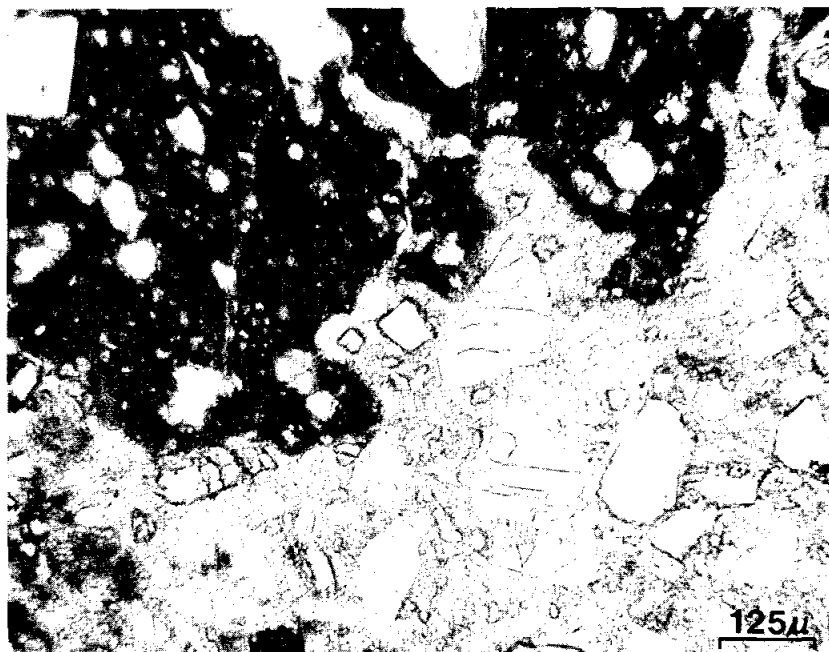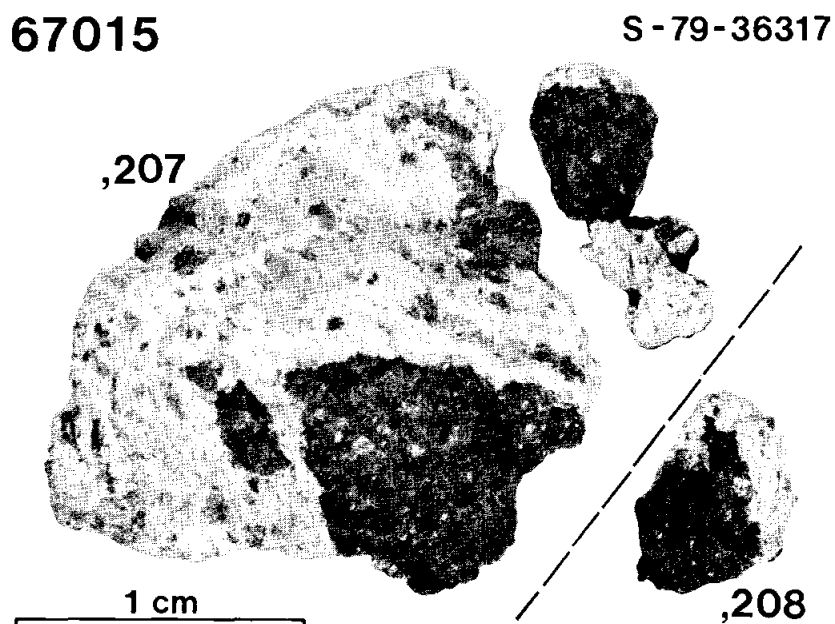
Fines from 67015,58.   A 17-gram sample of undocumented chips and fines, resulting from the disaggregation of the friable sample 67015,58, were sieved to produce samples 67015,164 to ,167. Basaltic clasts were handpicked from each of these samples and collected together to make sample 67015,168. (See Figures 19-23.)

The approximate distribution of grains sizes in 67015,58 are as follows:

67015,164	4-10 mm	4.11 g	25%
,165	2-4	3.02	18
,166	1-2	2.08	12
,167	< 1	6.62	40
,168	1-10	0.80	5
		16.63	

Figure 19. 67015,164 4-10 mm (4.0 g)

19 fragments including 5 predominantly of matrix that is moderately
coherent and contains small clasts of the dark gray vesicular and
the gray massive varieties; and 14 clast fragments, chiefly of the
gray massive type. Some have matrix attached; most do not.

S-79-31343

67015, 58

,164

1 cm
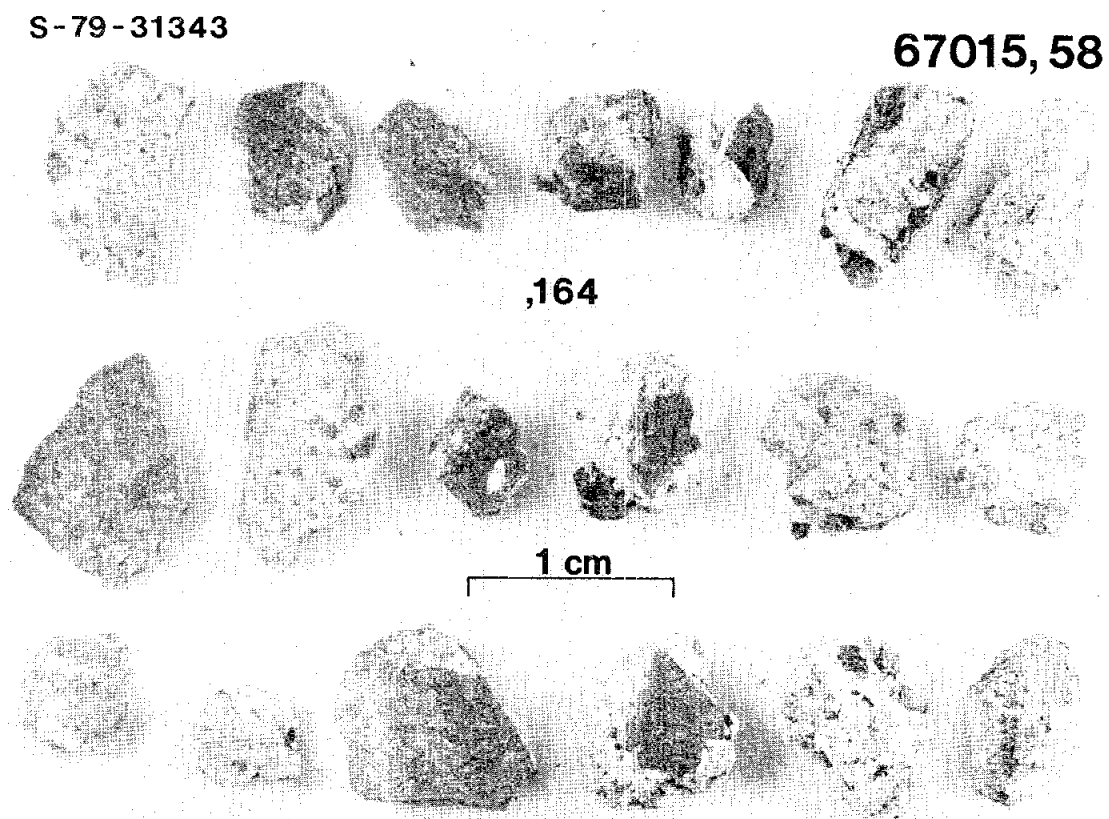
Figure 20. 67015,165 2-4 mm (3.02 g)

About 50% of these particles are of coherent matrix and 50% are clasts
of the dark gray or massive gray type.

67015, 58 1 cm S-79-31337

,165
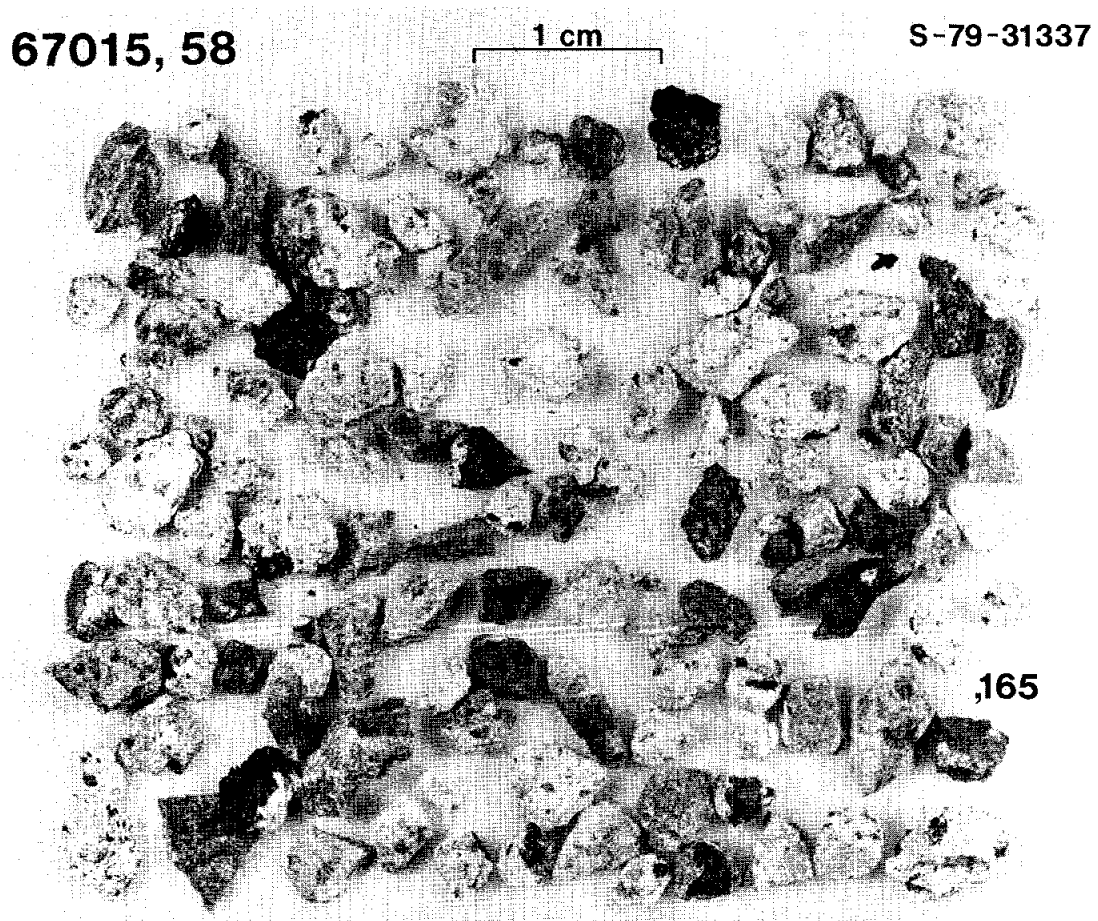
Figure 21. 67015,166 1-2 mm (2.08 g)

These materials include monomineralic fragments and, except for
basaltic particles which have been picked out, the full range of
matrix and clast types.

S-79-31344 1 cm ,166 67015, 58
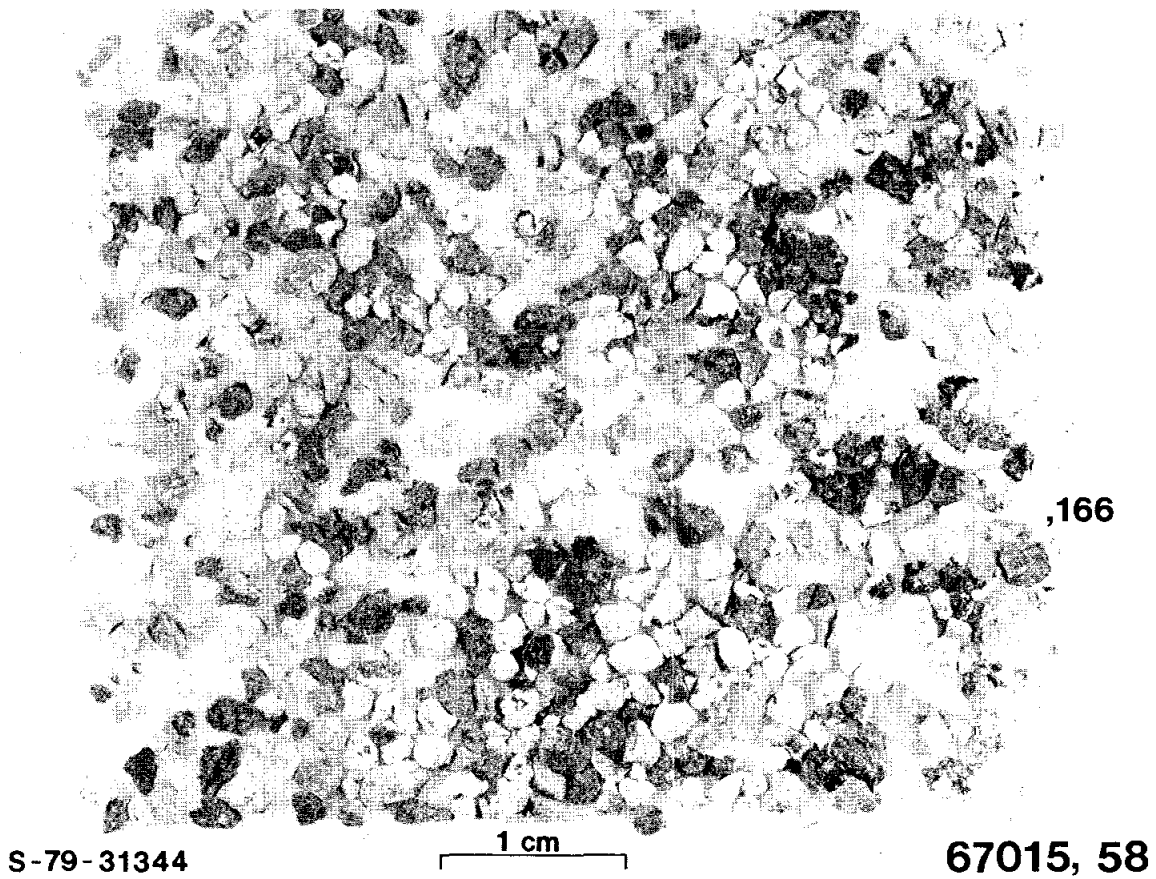
Figure 22. 67015,167 <1 mm (6.62 g)

Unpicked fine-fines of all the breccia materials.

S-79-31342

,167

67015,58
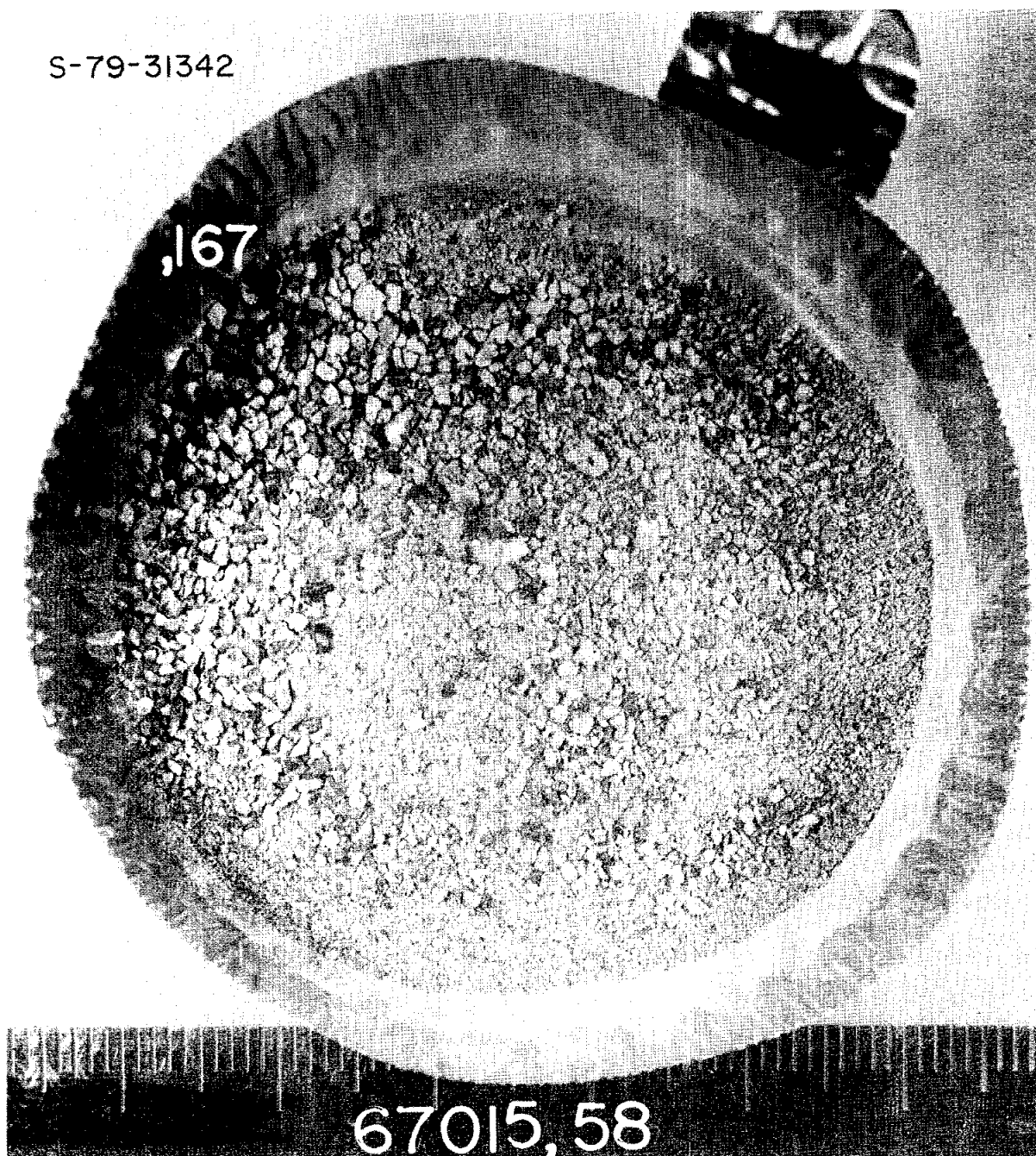
67015,168 consists of particles, handpicked from samples 67015,164 to ,166. These include coarse monomineralic fragments of olivine, pyroxene and plagioclase, and lithic clasts with igneous textures. Some are gray, sugary (noritic) crystallines and one or two are coarse anorthosites, but most are yellowish "basalts" ranging from coarse to fine-grained. A few of the particles are dark gray rinds with "basaltic" inclusions or crusts.

Five particles from 67015,168 were numbered separately 67015,200 - ,204 and stored for future study. 67015,200 is very friable (now in at least 2 pieces), coarsely crystalline, and usually rich in opaques, including one large metal grain, for samples from this breccia. 67015,201 and ,202 are friable to coherent basaltic particles with an average or higher than average percentage of mafics and opaques. 67015,203 is an anorthositic fragment; 67015,204 is a basaltic crust on a rind of dark matrix breccia.

Figure 23. Monomineralic and Lithic fragments hand picked from sample ,168.
Fragments ,200 to ,204 were numbered separately and set aside
for study.

S-79-35891

67015, 168

,168

,200

,201

,202

,203

,204
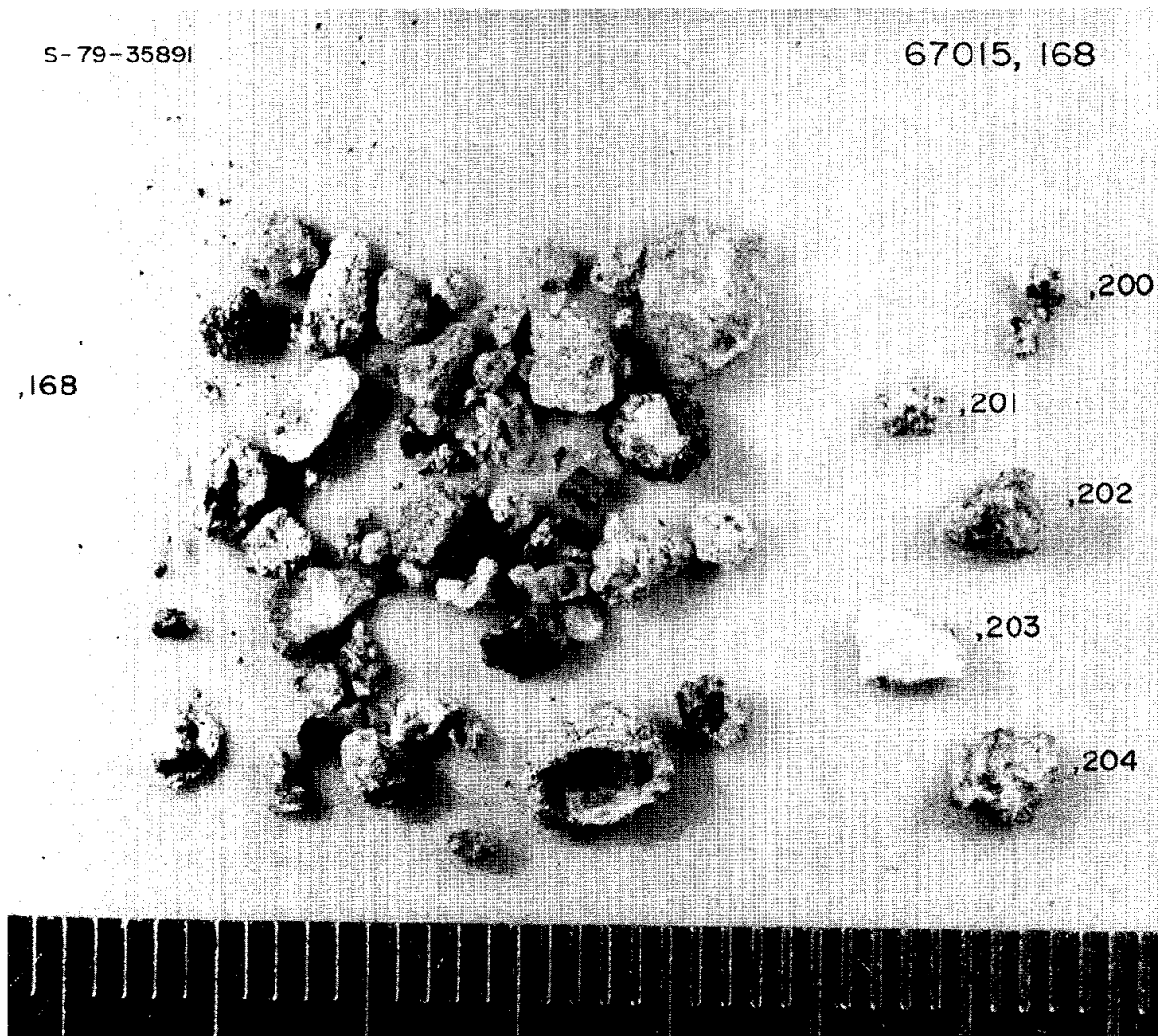
67015,126 and its subsamples. A 53.4-gram sample of undocumented chips and fines from 67015,0 was sieved on April 5, 1979, producing subsamples 67015,170-174. Figures 24 to 27 illustrate the coarser fractions. Individual photographs of the main portions of 2-4 mm and fine fractions are unenlightening and so are not included.

Samples 67015,173 (2-4 mm; 4.6 g) and 67015,174 (2-4 mm; 4.9 g) were separated by hand to obtain approximate proportions of coherent matrix fragments (,173) and of tough, aphanitic gray clasts (,174). These fractions are shown in Figure 24.

The distribution of grain sizes in 67015,126 is as follows:

67015,170	> 1 cm	2.80 g	5%
,171	4-10 mm	6.76	13
,172	2-4	0.56	
,173	2-4	4.66	19
,174	2-4	4.96	
,175	1-2	9.43	18
,176	< 1	23.35	45
		52.16	

Figure 24.   67015,126 and its subsamples.

S-79-31327
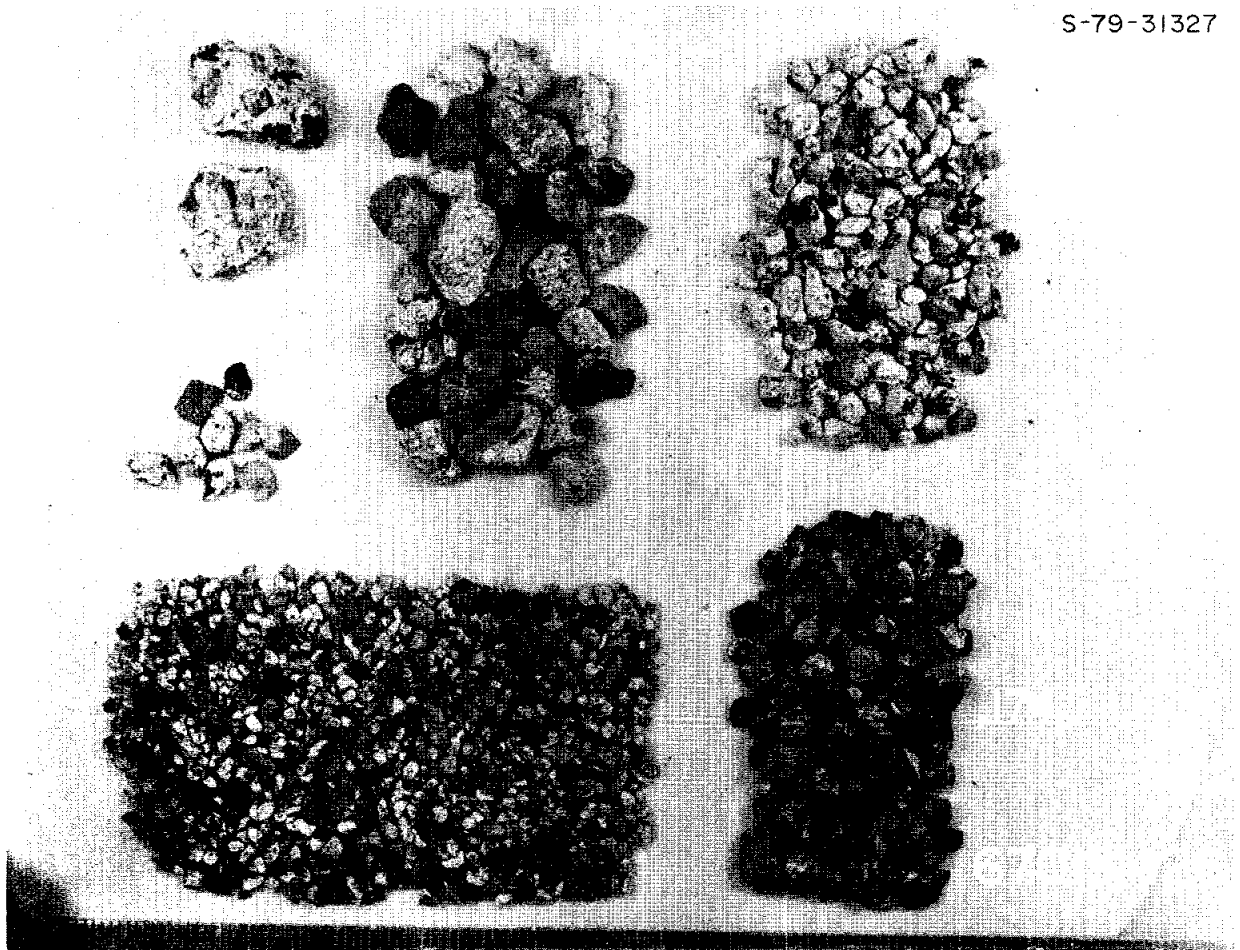
Figure 25. 67015,170 >1 cm (2.8 g)

Two chips predominately of matrix with 4 irregular patches of dark gray, vesicular clast material and one conspicuous medium-gray, massive clast. The clast (left center in Fig.) is loosely held in the friable matrix. Adjacent to it is a small clast of basaltic texture.

67015, 126   **S-79-31328**

,170
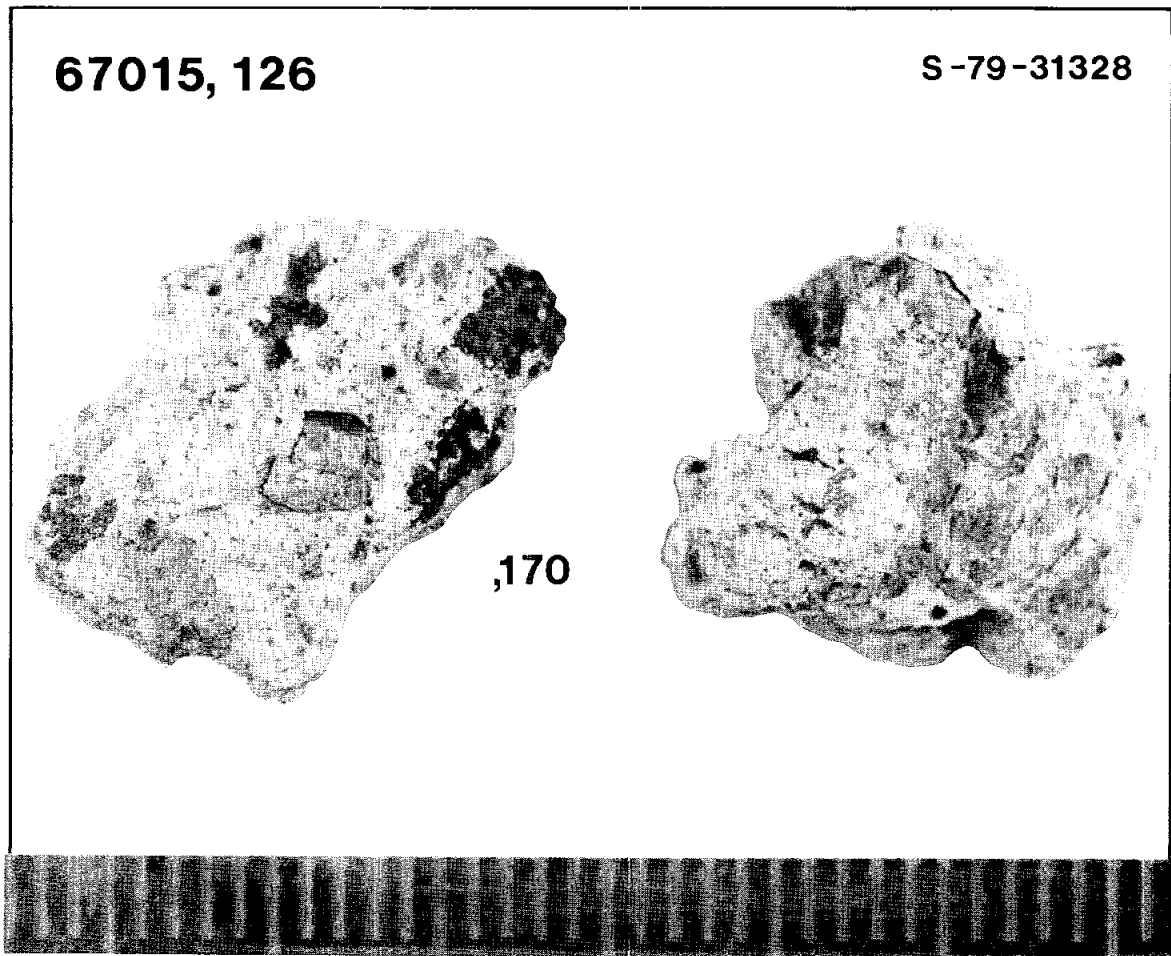
Figure 26. 67015,171 4-10 mm (6.7 g)

This sample consists of 36 fragments: 18 of them are mainly of friable
to moderately coherent matrix containing dark gray and medium gray clasts;
the remaining 18 are of tough, massive clast material. Most of these
fragments are aphanitic and featureless but one (left center in Fig.) is a
strongly annealed breccia with a variety of dark and light clasts.

S-79-31329

,171
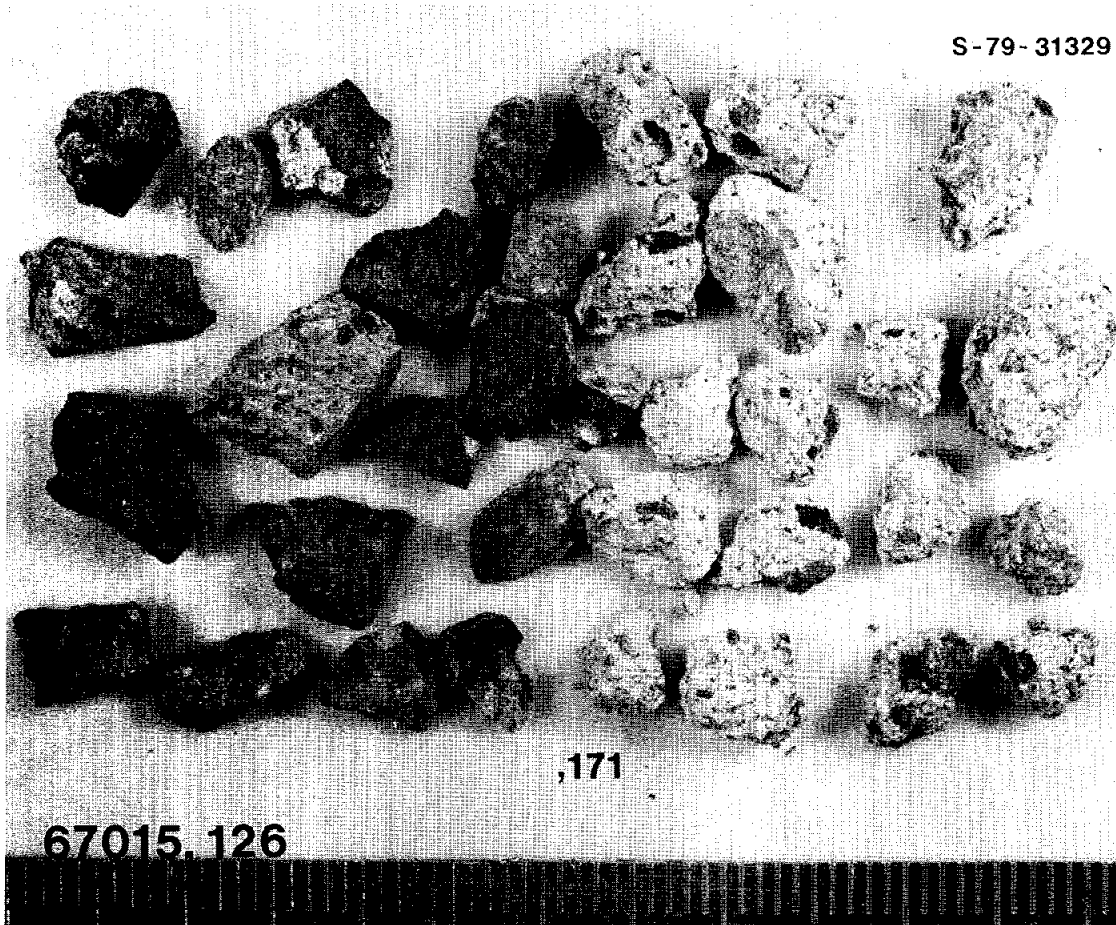
67015,126

Figure 27. 67015,172 2-4 mm (0.56 g)

Nine handpicked fragments including 3 that are mainly annealed matrix,
3 that are predominantly of dark gray, vesicular clast material, and 4
that are massive gray aphanites. One of the latter (upper left in Fig.)
consists partly of a mass of translucent plagioclase.

S-79-31330

,172
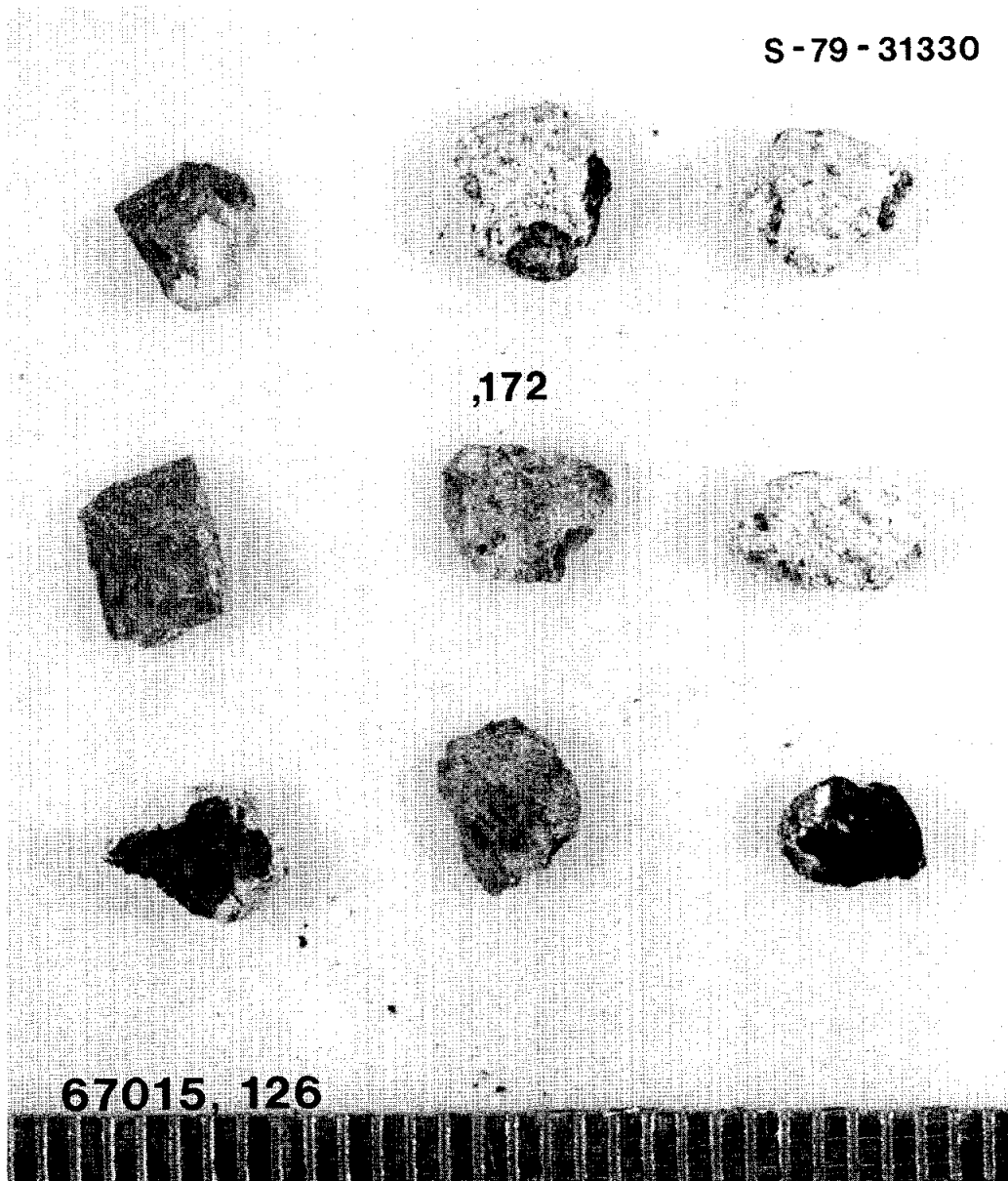
67015,126

<u>67015,62 and its subsamples</u>. A 44.3-gram sample of band saw fines
from the cutting of ,0 was sieved to produce samples   67015,179 to ,184
and ,191. Sample ,183 consists of crystalline particles selected for thin
sectioning.

The 2-4 mm material was handpicked into four subsamples: 67015,180
consists of matrix fragments; ,181 of dark gray, vesicular clasts with
attached matrix; ,182 of angular gray, aphanitic clast fragments. The
general character of these fractions is shown in Figure 28. 67015,183 is
a picked sample of crystallines and anorthosites (Figure 30).

The two finest fractions are 67015,184, 1-2 mm (6.544 g) and 67015,191,
1 mm (28.935 g). Both samples are unpicked. The size distribution in
this sample is:

,179	4-10 mm	2.24 g	5%
,180	2-4	1.40	
,181	2-4	0.71	12
,182	2-4	2.64	
,183	2-4	0.79	
,184	1-2	6.54	1
,191	< 1	27.93	66
		42. 25	

Figure 28.   67015,62 and its subsamples.

45
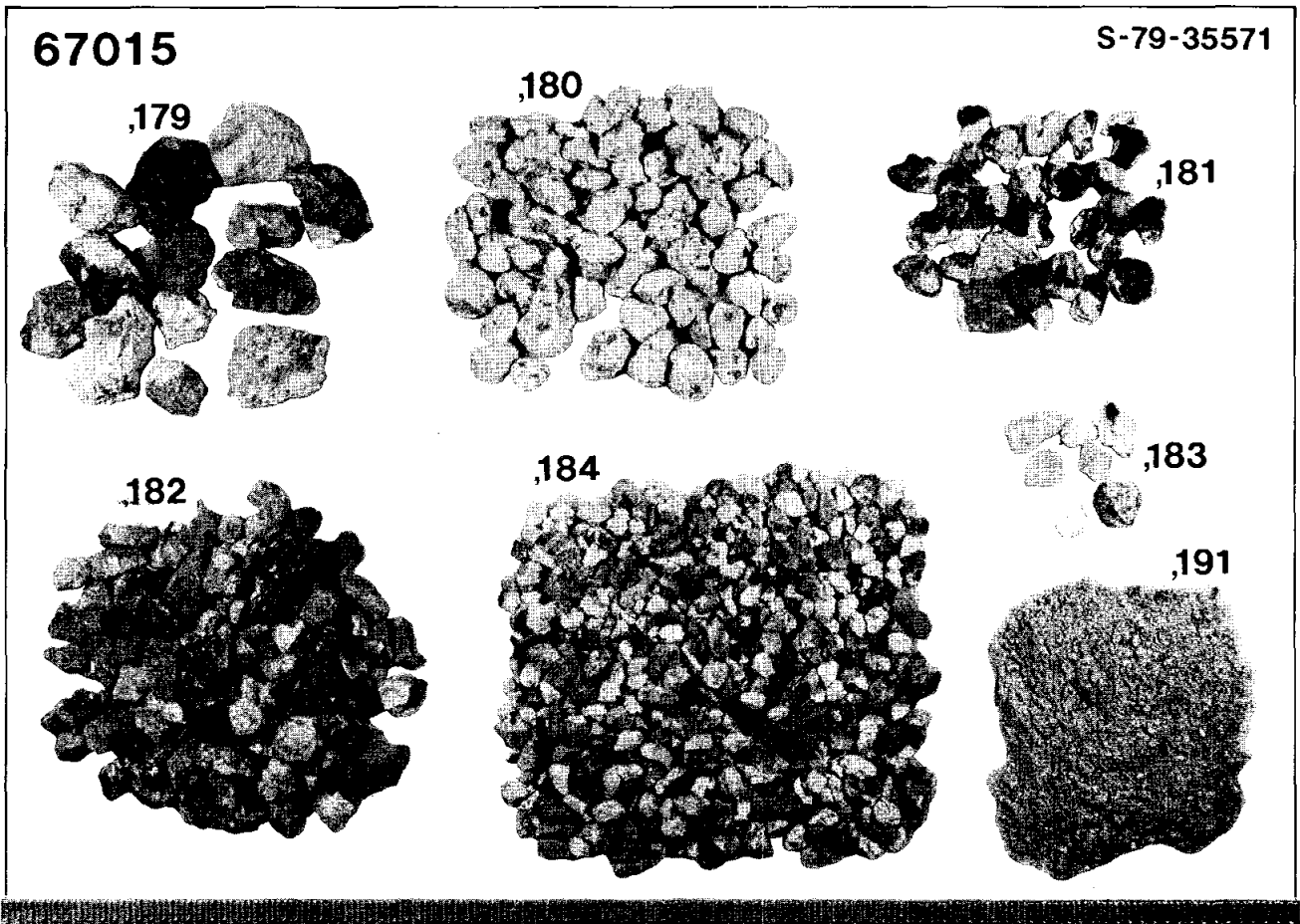
Figure 29. 67015,179 4-10 mm (2.247 g)

13 fragments including 3 that are chiefly of coherent matrix, 3
anorthositic clasts, 1 dark gray, vesicular clast, and 6 massive
gray, aphanitic clast fragments.

67015, 62   S-79-35766
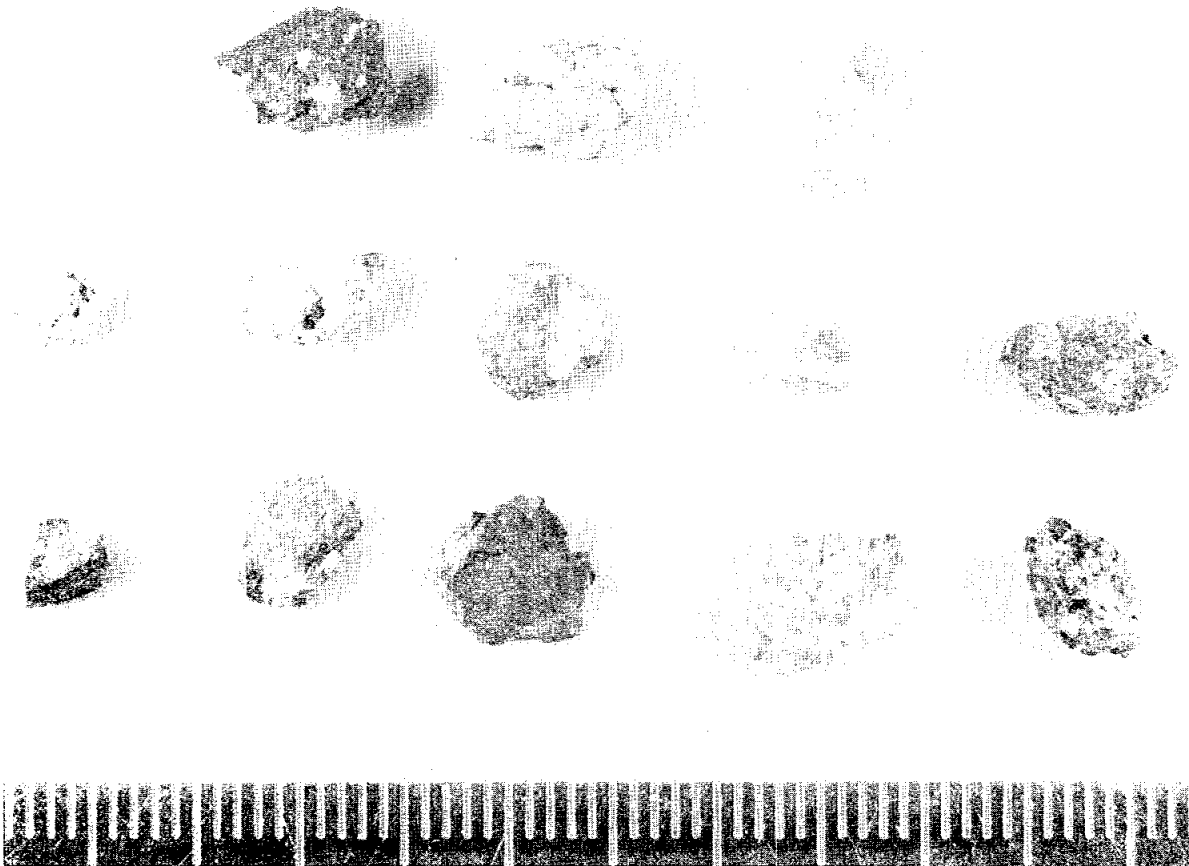
Figure 30. 67015,183 2-4 mm (0.79 g)

Seven crystalline particles selected for further study. Three are
anorthosites, two are gray-yellow, fine-grained, sugary crystallines,
and one is a gray sugary clast.
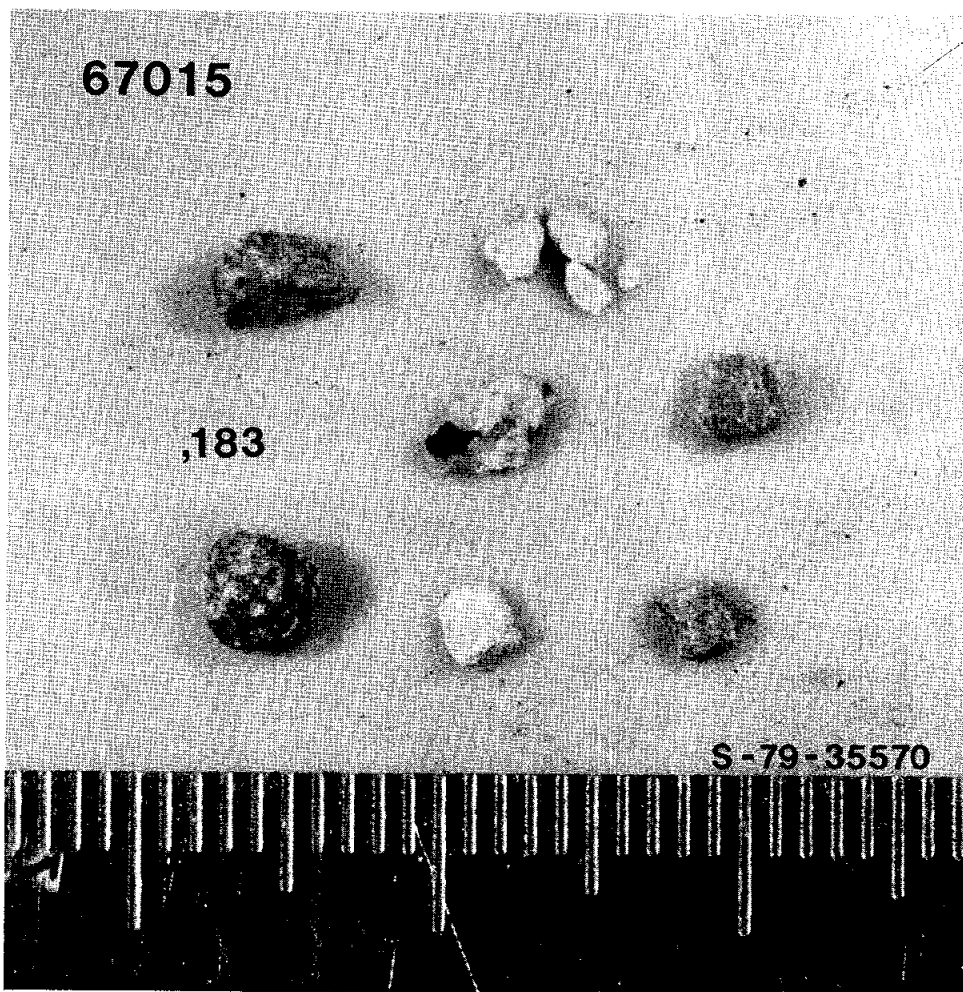
67015,179 and its subsamples. Five of the 13 4-10 mm fragments in 67015,179 were picked out and chipped for thin sections and chemical analyses. Figures 31 to 35 illustrate the particles and thin sections. The numbers and weights are as follows:

4-10 mm	Wt.G.	Subsample Potted Butt	Polished Thin Section	Figure
67015,185	0.24	,194	,211	31
,186	0.11	,195	,232	32
,187	0.22	,196	,212	33
,188	0.22	,197	,213	34
,189	0.18	,198	,214	35

Figure 31.   67015,185 and part of thin section 67015,211.

A.   A tough fragment of a fine-grained, light colored crystalline that
     would be mapped as lithology GC.

B.   This is recrystallized material with the bulk composition of a
     gabbroic anorthosite and a texture approaching granulitic impactite.
     Abundant small euhedral olivines occur in a groundmass of plagioclase
     crystals.   The plagioclases are of all sizes from a few μm to over 400
     μm; their grain boundaries approach but have not achieved the 120° angles
     of a fully recrystallized granulite.

A.
,185

B.

125μ
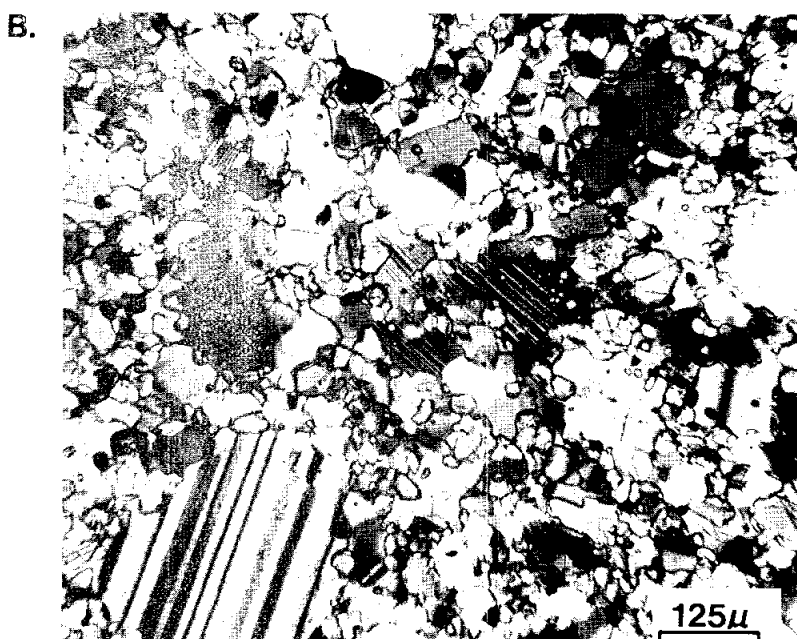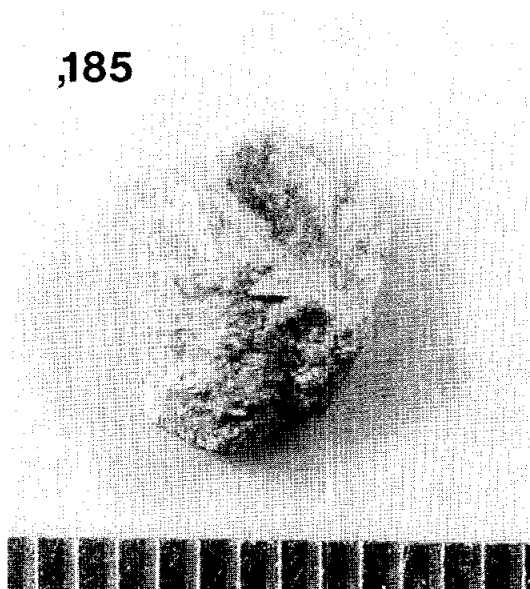
Figure 32.   67015,186 and thin section 67015,232.

A.   A 7-mm fragment of translucent plagioclase which appears to consist
     of only one or two crystals.

B.   The thin section reveals two large plagioclase crystals that have
     been partially maskelynitized to a leafy, randomized texture. The
     two crystals are indicated by domains with different average extinction
     orientations. The dark horizontal streak through the middle consists
     of glass separating the two domains. (Cross-polarized light.)
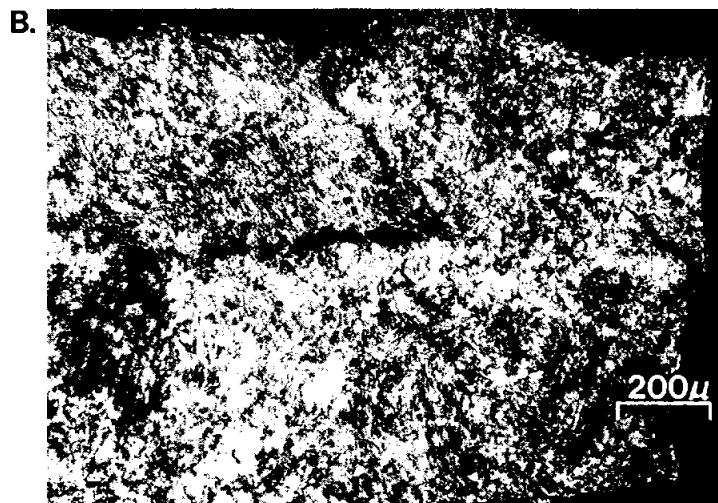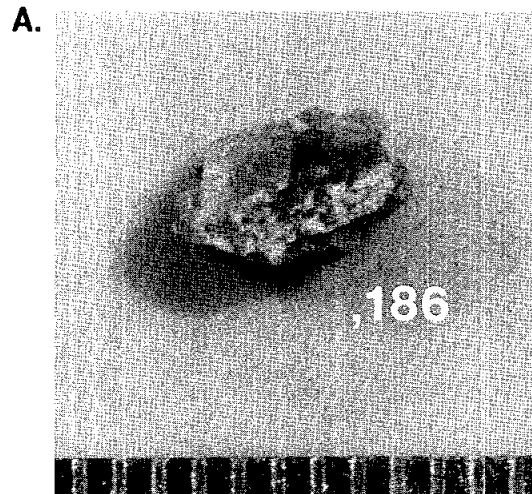
Figure 33. 67015,187 and two view of thin section 67015,212.

A. A fragment of massive gray (G-type) clast material. It is very fine-grained to aphanitic with tiny, sparse vesicles and one conspicuous light colored clast.

B. Views of thin section 67015,212 in plane and cross-polarized light.
and To the left is a fine grained domain typical of the rock as a whole.
C. The groundmass is recrystallized and rich in small clasts, chiefly of plagioclase with gradational borders, plus some large, undigested plagioclase fragments (upper left). At the right is a coarser re-crystallized polymict material rich in opaques, mafics with resorbed boundaries, and plagioclase clasts.

A.
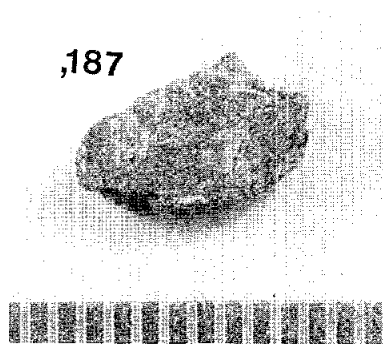
B.
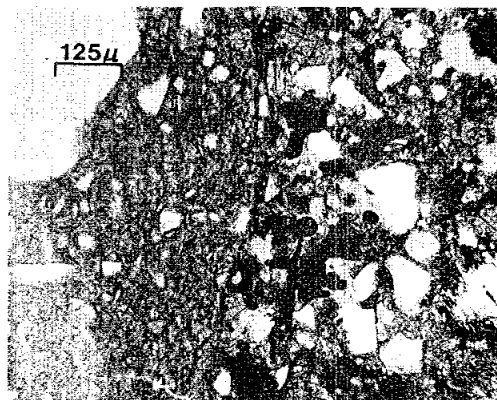
C.

Figure 34. 67015,188 and thin section 67015,213.

A. A tough, angular fragment that is obviously a recrystallized light
matrix breccia. Such materials are similar in color to the rock
matrix and are generally mapped as matrix although they might more
appropriately be considered clasts.

B. The thin section shows a polymict breccia with a very fine grained
groundmass. The lower part of the section illustrates a large
coarsely crystalline clast with plagioclase crystals in poikilitic
pyroxene. (Cross polarized light.)

A.

B.
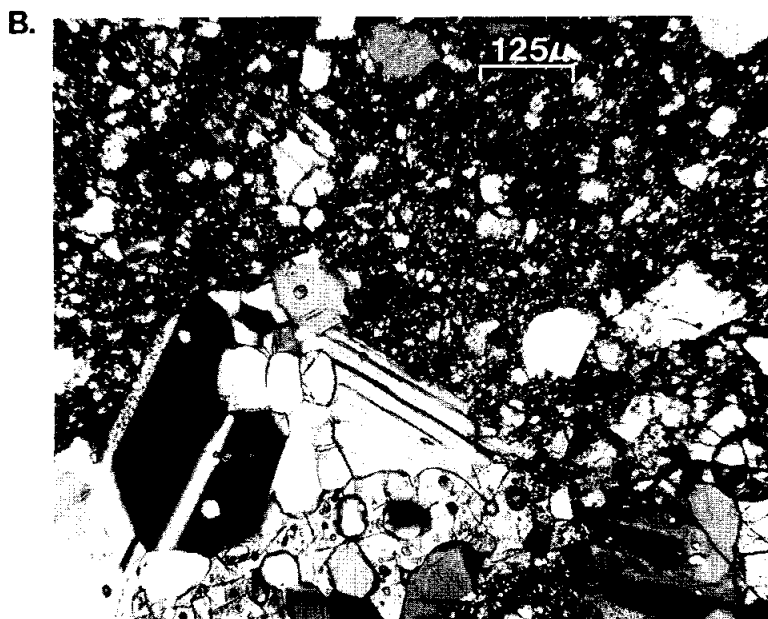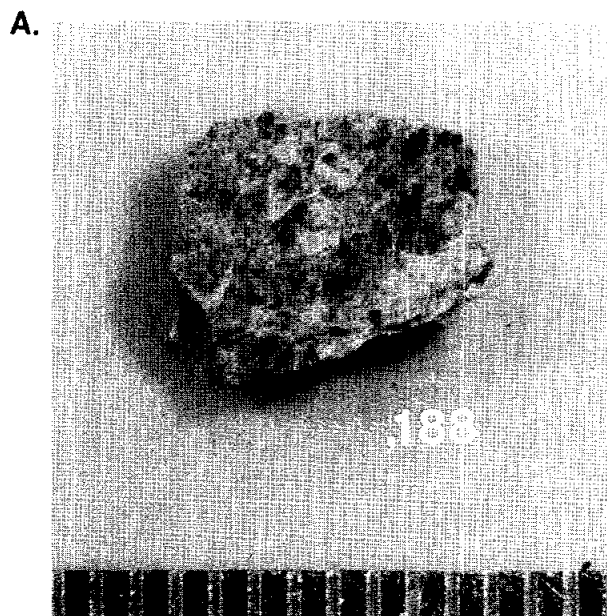
Figure 35. 67015,189 and part of thin section 67015,214.

A. A typical fragment of coherent matrix including irregular lobes of
   dark, vesicular material.

B. The thin section shows porous light matrix breccia incorporating
   dark lenses and rinds of dark, chestnut brown devitrified glass.
   Although the glass encloses certain lithic clasts it is markedly
   more vitric and less clast-rich than typical dark matrix breccia.
   (Plane polarized light.)

A.

,189

B.

125µ
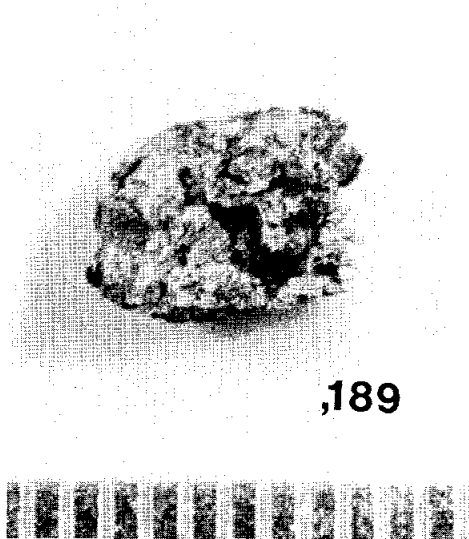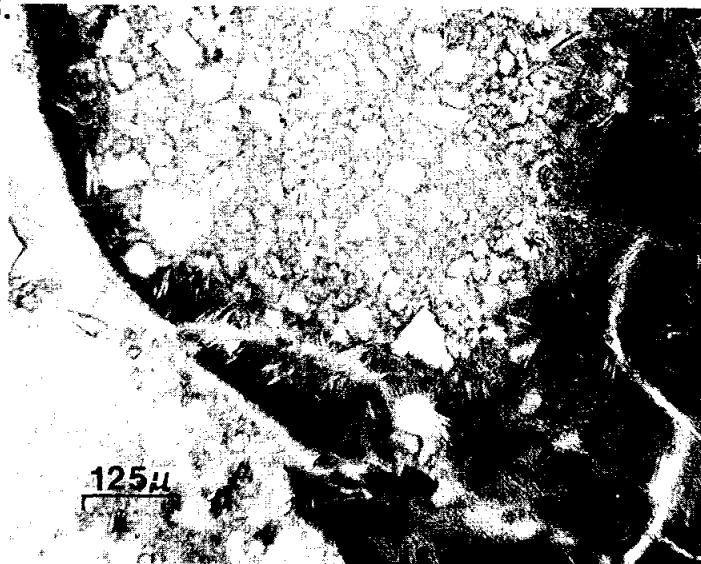
Literature Survey

Petrography. No systematic studies have been made of this rock although numerous thin sections and probe mounts have been available since the return of the Apollo 16 mission. It is clear from macroscopic examination that 67015 is polymict and inhomogeneous on a centimeter scale. In thin section 67015,88 Juan et al. (1974) described two zones, one consisting of 30% matrix and 70% lithic clasts, the other of 60% matrix, 5% lithic clasts and 35% mineral clasts. They calculated an overall composition of 30% lithic and 25% mineral clasts in a fine grained glassy matrix. Among the lithic clasts they found that 40% are preexisting breccias, 40% are anorthosites, 13% are non-mare basalts, and 2% are gabbros. The authors did not describe the mineralogy, texture, or grain size of the basalts and gabbros. They commented that the thin section reveals three generations of brecciation and annealing.

McGee et al. (1979) describe 67015 as a light-matrix breccia with an unrecrystallized matrix predominantly of plagioclase with minor mafic and opaque minerals, rare spinel grains, and orange-brown glass. The matrix is porous with intergranular voids, non-connecting veinlets and sparse vugs.

These authors cite the following modal analysis for the thin section 67015,74:

	Vol. %
Matrix (<39 μm)	55.35
Clasts (>39 μm)	44.65
	100.00
Mineral	
Plagioclase	12.39
Mafic	0.50
Devitrified glass	tr
Lithic	
Fragmental breccia	4.77
Crystalline breccia	17.04
Granulitic anorthosite	2.80
Gabbroic anorthosite	7.13

Their olivine analyses cluster at about Fo_{80-83} and Fo_{65-72}. A few pyroxene analyses show pigeonites ($En_{62-82}Wo_{3-6}$) and augites ($En_{43-53}Wo_{40-46}$). No plagioclase compositions are listed.

Among the lithic clasts are crystalline matrix breccias in which mineral fragments (mainly plagioclase) and rare lithic fragments occur in a matrix of fine-grained pyroxene and plagioclase. Other clasts have mineral and lithic fragments in partially glassy matrixes. Some of these clasts are round or ovoid and resemble chondrules. Clasts of granulitic and cataclastic anorthosites are both common. McGee et al. (1979) observed two unusual clast types, one of which consisted of plagioclase, mafic grains, and opaque laths in a matrix of brown glass, and one is composed of plagioclase laths 0.2 mm long with interstitial mafic grains and glassy mesostasis. This clast resembled Apollo 16 sample 68415.

Chemical Composition. In a series of articles on the chemistry of highland rocks and their derivation as mixtures of three components (anorthosite, KREEP, and Mg-rich primary material) Wänke and his co-workers reported major, minor, and trace elements in 67015,106. The sample was a 1.2 gram piece of matrix including at least 1 small dark clast. The analytical results of Wänke et al. (1975) are as follows:

Major Element %	Method	67015,106 Breccia	Accuracy %
O	IFNAA	44.8	1
Mg	IFNAA	2.33	4
	XRF	-	
	av.	2.33	
Al	IFNAA	15.6	2
	XRF	-	
	av.	15.6	
Si	IFNAA	21.5	1
	XRF	-	
	av.	21.5	
Ca	IFNAA	10.4	7
	ITNAA	11.6	7
	XRF	-	
	av.	11.0	
Ti	IFNAA	0.29	5
	ITNAA	-	
	XRF	-	
	av.	0.29	
Fe	IFNAA	2.80	3
	ITNAA	2.85	2
	XRF	-	
	av.	2.83	

Minor Element ppm	Method		
Na	ITNAA	3840	3
P	XRF	-	
S	XRF	-	
K	ITNAA	686	5
	XRF	-	
	av.		
Cr	ITNAA	438	3
	XRF	-	
	av.		
Mn	ITNAA	392	2
	XRF	-	
	av.		

Trace Element	67015,106 Breccia	Accuracy %
Li ppm		
F ppm		
Cl ppm		
K ppm	686	5
Sc ppm	7.47	3
Co ppm	9.67	5
Ni ppm	110	7
Cu ppm	1.46	10
Zn ppm	3.6	10
Ga ppm	4.1	7
Ge ppm	0.03	10
As ppb	8.3	10
Se ppm	0.14	15
Br ppm		
Rb ppm	1.42	10
Sr ppm	195	7
Y ppm	14.5	10
Zr ppm	55	7
Nb ppm	4.1	10
Pd ppm	0.001	15
Cs ppm	0.051	15
Ba ppm	86.2	7
La ppm	4.90	3
Ce ppm	11.6	5
Pr ppm	1.7	10
Nd ppm	7.9	10
Sm ppm	2.14	3
Eu ppm	1.16	3
Gd ppm	2.6	10
Tb ppm	0.47	10
Dy ppm	3.1	5
Ho ppm	0.7	10
Er ppm	1.9	10
Yb ppm	1.79	3
Lu ppm	0.24	5
Hf ppm	1.67	5
Ta ppm	0.21	10
W ppm	0.40	10
Re ppb	0.3	10
Ir ppb	-	15
Au ppb	1.1	10
Th ppm	0.7	15
U ppm	0.22	7
Fe/Mn	72.2	
K/La	140	
Zr/Hf	32.9	
La/Hf	2.93	

Wänke et al. (1976) further discussed the nature of the Mg-rich primary
component, for which they had calculated a ratio of Fe/Mg = 0.6, in lunar
highlands rocks. When their analyses of 67015,106 and several other Apollo
16 samples yielded ratios of Fe/Mg = >1.0, they concluded that the Mg-rich
component in these rocks could not be wholly unaltered primary material; the
mafic materials of 67015 must have been through a magmatic differentiation
that has raised an originally low Fe/Mg <1 ratio.

These authors pointed out that several samples including 67015 correspond
chemically to the ferroan anorthosites described by Dowty et al. (1974).

In 67015,106 Wänke et al. (1977) reported 12.0 ± 3.3 ppm Vanadium.

<u>Meteoritic Components.</u> Hertogen <u>et al.</u> (1977), investigating meteoritic components in highlands rocks, analyzed 47 Apollo 16 samples inlcuding 31 from North Ray Crater. Their values for a fragment of matrix and a dark clast from 67015,104 are given below.

Their results showed that the matrix contains essentially zero meteoritic component. They favored the interpretation that the matrix is actually a mixture of siderophile-free cataclastic anorthosites and microclasts from a component they designate as Group 7--siderophile-poor materials rich in refractories--with a bulk moon-like composition. They suggest that Group 7 materials, which occur at 4 landing sites, may represent the last few impacts by fragmented remnants of the moon's original planetesimal population.

The dark clast in 67015,104 contains siderophiles that Hertogen <u>et al.</u> interpret as appropriate to Group 1H, which is found exclusively at the Apollo 16 site. Such materials show contamination either from the projectile that produced a 60-km crater called Unnamed B, or, possibly, from the one that sculptured the Nectaris Basin.

Trace Elements by RNAA	67015,104 Matrix	67015,104 Dark Clast
ppb		
Ir	1.78	19.9
Os	1.72	17.3
Re	0.150	2.03
Au	0.565	15.5
Pd	1.79	42.7
Ni	39	855
Sb	0.40	3.75
Ge	109	2230
Se	54.7	227
Te	≤35	21
Ag	1.67	3.56
Br	63.6	81.3
In	0.24	0.83
Bi	0.28	0.54
Zn ppm	10.2	5.6
Cd	0.73	4.0
Tl	0.37	1.19
Rb ppm	0.87	6.73
Cs	70.3	300
U	140	1319
Ir/Au	0.953	0.380
Group	7	1H

Carbon Content. Modzeleski et al. (1973) measured total carbon and carbonaceous gases in several Apollo 16 samples. 67015,33 gave the lowest values of every compound they analyzed for. In μg/g of carbonaceous gases evolved at 500°C, 67015,33 yielded CO = 0.0, CO_2 = 22.7, CH_4 = 0.3; at 1000°C, CO = 3.6, CO_2 = 0.6, and CH_4 = 0.1. Total carbon from these gases was 8.2 μg/g. The other Apollo 16 samples yielded from 2 to 8 times more carbon.

Carbon, Sulfur, and Metallic Iron Analyses. Kerridge et al. (1975) reported carbon and carbonaceous gas analyses as well as sulfur and iron contents of 67015. Their results are listed below.

Carbon abundances (C ppm) and isotopic values (% relative to PDB)

	CO_2	CO	CH_4	Comb.	Total	$\delta^{13}C$	CO_2	CH_4	$\delta^{13}C_{CH_4}$
67015,31	11	6	1	6	24	-19.3	19	(3.0)	-
,39	13	3	0	1	17	-17.9	9.7	(0.4)	-21.4

Sulfur abundances and isotopic values

	Hydrolysis S ppm	$\delta^{34}S$	Pyrolysis-composition S ppm
67015,31	221	-0.02	176
,39	139	-2.2	71

Metallic iron

	Fe° wt. %
67015,31	0.23
,39	0.47

Oxygen Isotopes. Clayton, Hurd, and Mayeda (1973) measured the following values of oxygen-18 in fractions of 67015,32, a 1.97-gram undocumented chip:

	Matrix	Plagioclase	Dark Clast
δO^{18} (SMOW)	5.64	5.73	5.64

They observed that plagioclase dominates the rock and is indistinguishable from that in Apollo 16 igneous rocks. They found no O^{18} enrichment resulting from the effects of particle bombardment such as occurs in the Apollo 16 soils and would be expected in a soil breccia. The authors suggest that the components of 67015 were not exposed at the lunar surface before lithification.

U-Th-Pb. Nunes et al. (1973) investigated the systematics of U, Th, and
Pb in Apollo 16 samples including the matrix and a dark clast of 67015. They
found that, because of its anorthositic character, the matrix contains
remarkably small amounts of all three elements in comparison with Apollo 16
igneous rocks and soils. The dark clast contained higher concentrations of
U, Th, and Pb (see list below). The matrix of 67015 is somewhat more highly
enriched in Pb relative to U than is the clast, but both samples plot on a
discordia line, along with some Apollo 16 metaclastic rocks, an igneous rock,
and a North Ray Crater soil, with intercepts of 3.99 and 4.47 b.y. The authors
suggest that the 4.47 b.y. intercept dates a major episode of lunar differ-
entiation that occurred about 180 m.y. after the moon's birth, and the 3.99
b.y. intercept dates the Imbrian impact.

Nunes and coworkers published the following data on 67015.

Concentrations (ppm)

	Wt. mg.	Run	U	Th	Pb	$^{232}Th/^{238}U$	$^{238}U/^{204}Pb$
67015,12	492	1	0.196	0.689	0.629	3.64	243.8
matrix	563	2	0.200	0.732	0.640	3.77	292.2
	200	3	0.208	0.800	0.657	3.98	225.9
67015,11	710	1	1.176	4.225	2.54	3.71	1039.0
clast	218	2	1.219	4.346	2.62	3.68	1097.0
	134	3	1.212	4.461	2.61	3.80	1073.0

Their article also included data on Pb isotopes.

Rosholt (1974) measured the isotopic composition of the thorium in
lunar samples. In solutions of samples obtained from the laboratory of M.
Tatsumoto and P. Nunes he reported the following results:

Sample	U (ppm)	Th (ppm)	$^{232}Th/^{238}U$ (atomic ratio)	$^{232}Th/^{230}Th$ (expected activity ratio)	$^{232}Th/^{230}Th$ (measured activity ratio)	$\dfrac{\text{Expected ratio}}{\text{Measured ratio}}$
67015,12 matrix	0.200	0.732	3.76	1.19	1.08	1.10
67015,11 clast	1.21	4.449	3.77	1.20	1.15	1.04

Tera and Wasserburg (1974) reviewed the available data on U-Pb systematics of terra rocks and replotted, on a U-Pb evolution diagram, all of the published data. They found a generally linear array of points despite a very broad range of sample types having no immediately apparent genetic relationship. Their analysis of the data revealed internal inconsistencies in some published results. They questioned the precision of the data on 67015 by Nunes et al. (1973).

<u>Xenon Isotopes</u>. Lightner and Marti (1974) reported the following xenon concentration and isotopic abundances, normalized to ^{132}Xe = 100, in 67015,14.

^{132}Xe (10^{-12}ccSTP/g)	^{124}Xe	^{126}Xe	^{128}Xe	^{129}Xe	^{130}Xe	^{131}Xe	^{132}Xe	^{134}Xe	^{136}Xe
1.4	39.5	66.3	99.9	134.4	67.8	248	100	36.2	34.2

They discovered, in 14321 and several Apollo 16 light matrix breccias, a trapped component of Xe with a composition more strongly resembling that of terrestrial atmospheric xenon than of solar xenon. Most of this trapped component evolves after the temperature is raised to 900°C. After a series of analyses by different procedures the authors concluded that the trapped xenon is not a contaminant but is of lunar origin. It occurs in low abundance in breccia 67015.

Exposure Ages. Marti, Lightner, and Osborn (1973) measured ^{81}Kr-^{83}Kr in 67015,14, a 0.25-gram interior chip, and calculated an exposure age of 51 ± 5.0 m.y. Two other rocks from Station 11 (67915 and 67075 yielded exposure ages of 48.6 ± 4 and 48.5 ± 5.5 m.y. Marti et al. (1973) concluded that the impact event, which excavated North Ray Crater, occurred 48.9 ± 1.7 m.y. ago.

Macdougall et al. (1973) examined the irradiation history of lunar and meteoritic breccias and found that neither the olivine nor plagioclase grains in the matrix of 67015 retain any solar flare-produced particle tracks. They suggest that track-fading occurred during a heating event that raised the temperature of the breccia components to about 800°C (or to lower temperatures sustained over a relatively long period).

Hörz et al. (1975) investigated correlations between rock exposure ages and regolith dynamics. They concluded that rock 67015 has resided at depths of less than 10 cm in the regolith for the past 15 m.y.

Magnetic Properties. Tsay and Bauman (1975) measured the ferro-magnetic resonance of 67015,30, a 0.56 gram chip, and several other lunar samples. They found a correlation between the annealing temperatures of the metallic iron in the samples, as deduced by FMR spectral features, and metamorphic grade, as determined by thin section petrography. Their results indicated that the metallic iron in 67015 annealed to multidomian phases at temperatures of 800-1000°C. This conforms with the authors' assignment of 67015 to the class of high grade metamorphic breccias described by Warner (1972) for Apollo 14 rocks.

Brecher (1977) found 67015,42, a 12 gram documented chip, to give unreliable results either because the natural magnetic remanence and bulk magnetic susceptibility are too low to permit detection of magnetic anisotropy of 1 to 10% or because the shape of the sample was unsuitable for relating magnetic and petrofabric features.

Hohenberg et al. (1978) compared observed with predicted rates of production of cosmogenic noble gases in samples from Cone Crater (Apollo 14) and North and South Ray Craters (Apollo 16). The rocks selected, including 67015, are small, well documented samples with simple exposure histories, low shielding depths, and exposure ages of about 50 million years or less, measured by the ^{81}Kr method. The following data were reported on 67015,14 for argon, krypton, and xenon.

Comparisons of observed and predicted cosmogenic gases in 67015,14: shielding depth 1-2 g/cm^2, exposure age 51.1 m.y. (A 20% uncertainty in elemental abundances and a surface erosion rate of 0.39 g/cm^2-m.y. are assumed. Predicted cosmogenic production rates uncorrected for erosion are shown in parentheses.)

Argon

Target Chemistry		
	K	0.15
	Ca	11.0
	Ti	0.29
	Fe	2.83

^{38}Ar (Obs.)   1.1 ± .1
^{38}Ar (Pred.)
(x 10^{-9}cm^{3}STP/g-m.y.)   1.25 - 1.21 ± .24
                                (2.5 - 1.8)

Predicted Cosmogenic Composition

36 = 0.666 - 0.668
38 = 1.000
40 = 0.011 - 0.011

Krypton

		ppm
Rb	3	
Sr	150	
Y	87	
Zr	260	
(Br	0.4	

^{83}Kr (meas.) 1.21 ± .18
^{83}Kr (pred.) 0.825 ± .17
                 (1.07 - 1.28)
^{81}Kr (meas.) 2.19 ± .35
^{81}Kr (pred.) 2.07 - 2.35
                 ±20%

Observed Cosmogenic Spectrum

78 = 0.218 ± .003
80 = 0.566 ± .010
81 = .0038 ± .0006
82 = 0.784 ± .009
83 = 1.000
84 = 0.357 ± .015

Predicted Cosmogenic Spectrum

78 = 0.211 - 0.216
80 = 0.710 - 0.730
81 = 0.0036 - 0.0038
82 = 0.867 - 0.874
83 = 1.000
84 = 0.568 - 0.564

Xenon

		ppm
Ba	220	
La	22	

^{126}Xe (meas.)   0.22 ± .03
^{126}Xe (pred.)   0.24 ± .05
(x 10^{-12}cm^3/g-m.y.)   (0.26)

Observed Cosmogenic Spectrum

124 = 0.593 ± .016
126 = 1.000
128 = 1.46 ± .20
      1.54 ± .12
129 = 1.70 ± .40
130 = 0.86 ± .12
131 = 3.85 ± .96
132 = 0.50 ± .34
134 =   -

Predicted Cosmogenic Spectrum

124 = 0.671 ± .017
126 = 1.000
128 = 1.376 ± .022
129 = 1.543 ± .030
130 = 0.565 ± .042
131 = 3.06 ± .12
132 = 0.421 ± .034
134 = 0.028 ± .002

References

Brecher, A. (1977) Interrelations between magnetization directions, magnetic fabric and oriented petrographic features in lunar rocks. Proc. Lunar Planet. Sci. Conf. 8th, pp. 703-723.

Clayton, R.N., Hurd, J.M., and Mayeda, T.K. (1973) Oxygen isotopic composition of Apollo 15, 16, and 17 samples, and their bearing on lunar origin and petrogenesis. Proc. Lunar Sci. Conf. 4th, pp. 1535-1542.

Dowty, E., Prinz, M., and Keil, K. (1974) Ferroan Anorthosite: A widespread and distinctive lunar rock type. Earth and Planet. Sci. Lett., Vol. 24, pp. 11-25.

Hertogen, J., Janssens, M.-J., Takahashi, H., Palme, H., and Anders, E. (1977) Lunar basins and craters: Evidence for systematic compositional changes of bombarding population. Proc. Lunar Planet. Sci. Conf. 8th, pp. 17-45.

Hodges, C.A., Muehlberger, W.R., and Ulrich, G.E. (1973) Geological Setting of Apollo 16. Proc. Lunar Sci. Conf. 4th, pp. 1-25.

Hohenberg, C.M., Marti, K., Podosek, F.A., Ready, R.C., and Shirck, J.R. (1978) Comparisons between observed and predicted cosmogenic noble gases in lunar samples. Proc. Lunar Planet. Sci. Conf. 9th, pp. 2311-2344.

Horz, F., Gibbons, R.V., Gault, D.E., Hartung, J.B., and Brownlee, D.E. (1975) Some correlation of rock exposure ages and regolith dynamics. Proc. Lunar Planet. Sci. Conf. 6th, pp. 3495-3508.

Juan, V.C., Chen, J.C., Huang, C.K., Chen, P.Y., and Wang Lee, C.M. (1974) Petrology and chemistry of some Apollo 16 and lunar samples. Lunar Science V, The Lunar and Planetary Institute, Houston, pp. 394-396.

Kerridge, J.F., Kaplan, I.R., and Petrowski, C. (1975) Light element geochemistry of the Apollo 16 site. Geochim. Cosmochim. Acta, Vol. 39, pp. 137-162.

Lightner, B.D. and Marti, K. (1974) Lunar trapped xenon. Proc. Lunar Sci. Conf. 5th, pp. 2023-2031.

MacDougall, D., Rajan, R.S., Hutcheon, I.D., and Price, P.B. (1973) Irradiation history and accretionary processes in lunar and meteoritic breccias. Proc. Lunar Sci. Conf. 4th, pp. 2319-2336.

Marti, K., Lightener, B.D., and Osborn, T.W. (1973) Krypton and xenon in some lunar samples and the ages of North Ray Crater. Proc. Lunar Sci. Conf. 4th, pp. 2037-2048.

McGee, P.E., Simonds, C.H., Warner, J.L., and Phinney, W.C. (1979) Introduction to the Apollo Collections. Part II: Lunar Breccias. NASA, Lyndon B. Johnson Space Center, Houston, Texas 77058.

Modzeleski, J.E., Modzeleski, V.E., Nagy, B., Nagy, L.A., Sill, G.T., Hamilton, P.B., McEwan, W.S., and Urey, H.C. (1973) Types of carbon compounds examined in Apollo 16 lunar samples by vacuum pyrolysis-mass spectrometry and by photo-electron spectroscopy. Lunar Science IV, The Lunar and Planetary Institute, Houston, pp. 531-533.

Nunes, P.D., Tatsumoto, M., Knight, R.J., Unruh, D.M., and Doe, B.R. (1973) U-Th-Pb systematics of some Apollo 16 lunar samples. Proc. Lunar Sci. Conf. 4th, pp. 1797-1822.

Rosholt, J.N. (1974) Isotopic composition of thorium in lunar samples. Lunar Science V, The Lunar and Planetary Institute, Houston, pp. 648-650.

Tera, F., and Wasserburg, G.J. (1974) U-Th-Pb systematics on lunar rocks and inferences about lunar evolution and the age of the moon. Proc. Lunar Sci. Conf. 5th, pp. 1571-1599.

Tsay, F.D. and Bauman, A.J. (1975) Ferromagnetic resonance as a geothermometer for probing the thermal history of lunar samples. Lunar Science VI, The Lunar and Planetary Institute, Houston, pp. 821-823.

Ulrich, G.E. (1976) Field Geology of North Ray Crater. Chapter E2 in Ulrich, G.E. Hodges, C.A., and Muehlberger, W.R. eds. (1979). Geology of the Apollo 16 Area, Central Lunar Highlands, U.S. Geol. Survey Open-file Report 79-1091.

Pieces ≥ 1 gram

Sample	Parent	Grams	Description
67015,18	0	1.90	Undocumented exterior chip
,19	0	1.00	Undocumented black chip
,29	16	4.82	Doc. chip
,32	16	1.97	Undoc. (Clayton)
,33	16	4.82	Undoc. (RSPL)
,36	16	1.87	Doc. chip
,42	17	12.09	Doc. chip (Simmons)
,43	17	3.86	Doc. chip (Fuller)
,44	17	2.73	Doc. chip (Gold)
,56	0	2.35	Doc. clast & matrix
,57	0	386.10	East end piece
,60	0	5.76	Located matrix & clast
,61	0	2.24	Doc. matrix & clast chip
,64	0	340.50	Middle of main mass
,105	35	2.05	2 chips (Rhodes)
,106	35	1.20	Chip (Wänke)
,108	7	5.26	Chips (Geiss)
,109	0	1.39	Doc. black clast chip
,111	0	12.45	Doc. chip & loc.
,116	0	2.11	Black clast & white matrix (Geiss)
,117	0	2.54	Black clast & white matrix (Geiss)
,123	0	1.00	Matrix chip
,125	0	2.36	Located matrix chip
,159	57	11.69	Large chips & fines
,161	58	43.98	Located matrix pieces
,162	58	31.14	Located matrix pieces
,205	163	7.86	Black & white chip
,206	163	5.99	White pitted chip
,207	163	2.61	Bandsaw chip
,210	161	1.34	Loc. chip
,216	158	7.25	Black clast pieces
,217	158	5.67	Black clast pieces
,218	158	3.27	Black clast pieces
,219	161	4.40	2 Loc. chips
,221	57	7.45	8 Black & white chips

Genealogical Chart for 67015